2002

Developments in high temperature superconductivity

Tania M. Silver
University of Wollongong, tsilver@uow.edu.au

A. V. Pan
University of Wollongong, pan@uow.edu.au

M. Ionescu
University of Wollongong, mionescu@uow.edu.au

M. J. Qin
University of Wollongong, qin@uow.edu.au

S. X. Dou
University of Wollongong, shi@uow.edu.au

9 Developments in high temperature superconductivity

T. Silver,* A. V. Pan, M. Ionescu, M. J. Qin and S. X. Dou

Institute for Superconducting and Electronic Materials, University of Wollongong, Northfields Eve., Wollongong, NSW 2522, Australia

1 Introduction

The past four years (1997–2001) have seen many exciting developments in high temperature superconductivity, most notably the discovery of the superconducting nature of magnesium boride in 2001 and the amazing critical temperatures of 52 K, then 117 K, achieved in 2000 by hole doping C_{60} fullerenes through incorporation into a field effect transistor (FET). Steady progress has also been made in understanding the recently discovered rutheno-cuprate superconducting ferromagnets. Theoretical work over this period has been focused on understanding the pseudogap in high temperature superconductors and on determining the mechanism behind superconductivity in MgB_2. Much attention has also been devoted to the rich and complex vortex behaviour found in both the older copper oxide high temperature superconductors and in MgB_2.

This has also been a period for technological progress. We highlight developments in the field of superconducting tapes and wires, including the considerable success achieved in making high critical current iron-clad MgB_2 tape. Second generation coated conductors have also become an important new field, because they provide a way of overcoming some of the disadvantages of tapes and wires. Small scale devices, such as SQUIDs and microwave filters, have been based on films of high temperature superconductors for some time, but larger scale applications are now coming closer to practical use. Superconducting power transmission cables cooled by liquid nitrogen are now in use in Copenhagen and Detroit.

2 New HTSC compounds

Although the period 1999 to 2001 saw the introduction of far fewer new copper oxide superconductors than the average in the previous decade, there was more than enough compensation in the discovery of the superconductivity of MgB_2 and the record high critical temperatures achieved in C_{60}. Although the various rutheno-cuprate families of superconductors were first reported as ferromagnetic and superconducting in 1997, most of the work to characterise them was done during this period. It is also notable that for the first time during this period molecular beam epitaxy (MBE) was used to grow novel high temperature copper oxide superconductors.

2.1 Magnesium boride

History. At the beginning of 1999 superconductors fell into two distinct groups, the low-T_c superconductors with critical temperatures T_c below 24 K and the high-T_c copper oxide compounds with T_c above 30 K. By 2001 a T_c of more than 40 K had been achieved in C_{60} fullerene compounds, but only in a quasi-2D system.[1] All high temperature bulk superconductors then known were still copper oxides. MgB_2 is a black, intermetallic, polycrystalline material that had been known since 1953 and was used in the commercial preparation of elemental boron.[2] It was not known to be superconducting until this property was accidentally discovered by Akimitsu and colleagues.[3] Furthermore, MgB_2 had a critical temperature of 39 K, 16 K above the previous low-T_c record. There was immediate interest both from the physics point of view and because of the possibility of technological applications. From the physics point of view, the interesting question is whether MgB_2 is a normal low temperature superconductor explained by BCS theory or whether it is something entirely new, an issue that is discussed in the theory section of this review. The technological interest has accelerated as many favourable properties, such as high critical current densities have been discovered. Buzea and Yamashita[4] have recently written a comprehensive review article surveying the great volume of literature on MgB_2 that has been recently published.

Preparation and material stability. Polycrystalline bulk material had been and still is grown by solid state reaction (Mg diffusion method), where the volatile Mg is sealed together with the boron and generally sintered between 650 °C and 1000 °C. It soon became obvious that the bulk synthesis needed to be optimised for superconducting purposes, to maximise the critical current J_c. Densities were typically far below the theoretical value of 2.63 g cm^{-3}, and the material was often porous and mechanically weak. High pressure during synthesis increases the density and improves J_c.[5–7] High pressure combined with high sintering temperatures above 800 °C also proved to be beneficial.[8–10] Texturing by hot deformation, however, to align the randomly oriented grains produced no anisotropy in the critical current density.[11]

Single crystals have only been grown in the submillimetre size with the methods used including vapour transport,[12] growth under high pressure in an Mg–B–N system,[13] and a solid–liquid reaction method,[14] but there has been greater success with films where the largest critical current densities (>10 MA cm^{-2}) have been achieved.[15] Thin films and tapes and wires are discussed in the applications section of this review.

Material stability is of great importance for technological applications. The superconducting properties of MgB_2 are subject to degradation by exposure to moist air and immersion in water. Aswal *et al.*[16] found that thin superconducting bridges (2 mm × 0.5 mm × 0.2 mm) became insulating after exposure to ambient atmosphere with humidity > 70%. Zhai *et al.*,[17] however, found no degradation in T_c in the case of 800 nm thin films that were immersed in water for up to 15 h. This indicates that at least a portion of the sample was not degraded. Fan *et al.*[18] investigated the thermal stability of MgB_2 and found that decomposition and desorption of Mg starts to occur in vacuum at temperatures above 425 °C.

Crystal structure. MgB_2 consists of alternating layers of boron and magnesium atoms in a hexagonal structure, as shown in Fig. 1. He *et al.*[19] analysed the crystal

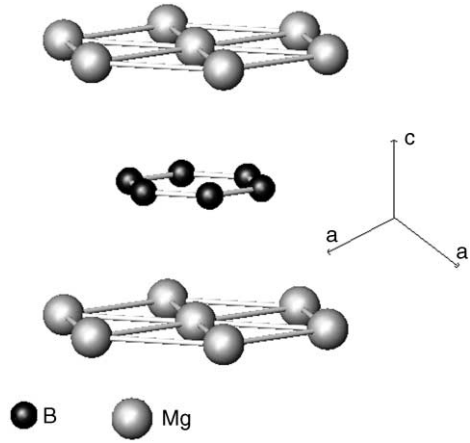

Fig. 1 MgB_2 consists of alternating hexagonal sheets of magnesium and boron atoms.

structure of MgB_2 using the Rietveld method. They found that the compound has hexagonal symmetry (space group *P6/mmm*) with the unit cell lattice parameters: a = 0.308136(14) nm and c = 0.351782(17) nm. Lee *et al.*[13] used X-ray diffraction analysis on their small single crystal samples and found that a = 0.30851(5) nm and c = 0.35201(5) nm. Similar conclusions on the crystal structure have been made on the basis of studies using high resolution transmission electron microscopy (HRTEM),[20] high resolution powder neutron diffraction[21] and electron energy loss spectroscopy.[22]

Studies of the grain structure in dense samples[20,23] have shown very good grain connectivity and regularly stacked grains. MgO and BO_x impurities have been reported at grain boundaries.[24] Zhu *et al.*[25] also reported unreacted Mg at grain boundaries, and a substantial presence of MgO as a second phase. They found that dislocations and stacking faults were preferentially located in the (001) plane.

Elastic constants. Cordero *et al.*[26] measured the dynamic elastic modulus of MgB_2. They were unable to find any unexplained anomalies that might be associated with lattice instabilities leading to an enhanced electron–phonon coupling (to explain the high T_c). This is in agreement with some theoretical calculations.[27] Calculations of the five elastic constants from density functional theory[28] also suggest that MgB_2 is less anisotropic than might be expected from the planar structure.

Pressure effects. The critical temperature of conventional BCS superconductors is reduced under pressure, and the same is true for MgB_2.[29,30] The rate of reduction is of the order of -1.6 K GPa^{-1}[31] comparable to theoretical calculations assuming BCS material.[32] Slightly different experimental values that are still compatible with BCS theory are reported by other workers,[33–35] possibly due to sample dependent effects. One group[36] reported a cusp in the T_c pressure dependence at 9 GPa.

An anisotropy in the compressibility has also been reported. The c axis decreases more rapidly with compression than the a axis, indicating that the Mg–B bonds are weaker than the Mg–Mg bonds.[30,37–39] Jorgansen *et al.*[39] also found higher c-axis

responses in the thermal expansion. The anisotropic compressibility and other aspects of behaviour under pressure have been theoretically modelled.[40,41] One group[42] has reported an isostructural transition at 30.2 GPa in a diamond anvil cell, marked by a 7% decrease in the unit cell volume and a split in the Raman spectrum. Goncharov *et al.*[38] also observed a shift with pressure in a Raman spectrum band.

Doped MgB_2 and related compounds. Various borides and borocarbides were known to be superconducting before the discovery of MgB_2, but only at low temperature, and some others have been found to be superconducting since. A comprehensive table of such compounds is included in ref. 4. It should be noted that the next highest critical temperature after MgB_2 is 23 K, which occurs in the borocarbide YPd_2B_2C.

1 Vacancies and doping into the B sublattice. As discussed in the theory section, band structure calculations[43–45] attribute the superconductivity of MgB_2 to metallic B states or more specifically to $p_{x,y}$-band holes in negatively charged boron planes. Such calculations imply that inducing vacancies in the boron sublattice, or fully or partially replacing boron by some other element, is counterproductive, because of a reduction in the density of states near the Fermi energy. Medvedeva *et al.*[46] predicted that doping MgB_2 with carbon would reduce the critical temperature. This is what is in fact observed experimentally. Carbon does substitute into the boron site, causing a decrease in the superconductivity and in the *a*, but not the *c*, lattice parameter.[47,48] Mehl *et al.*[49] predicted that it might be possible to overcome this problem and achieve a T_c of 50 K by combining C doping in the boron site with Cu doping in the Mg site. As described below, this cannot be achieved, because Cu will not incorporate into the MgB_2 lattice.

2 Vacancies or doping into the Mg sublattice. Since the superconductivity depends on holes it might be expected that n-type substitutions into the Mg site would have detrimental effects on the superconductivity, either eliminating it entirely or reducing the critical temperature depending on the element and the doping levels.[44,46,50] AlB_2 is not a superconductor. Slusky *et al.*[51] have found that partial substitution of Al for Mg in MgB_2 results in a loss of superconductivity, with T_c decreasing smoothly and vanishing at a 25% doping level. They attributed this to the greater electron concentration arising from Al doping and also to a structural transition.

Hole doping or isoelectronic doping appears more promising, but some workers[43,46] have found that hole doping does not increase the density of states near the Fermi level $N(E_F)$, while isoelectronic doping decreases the density of states. It was thus predicted for example that BeB_2 would be unfavourable for superconductivity,[46,49] although it is isoelectronic with MgB_2, on the basis of differences in the lattice parameters leading to a lower $N(E_F)$. Chen *et al.*[52] have calculated bond ionicities in the diborides and have found that the greatest value is found in MgB_2, suggesting that this has something to do with its superior performance, since the other compounds are either not superconducting, or only superconducting at very low temperatures.[53]

No one has managed to dope Na or Ca into the Mg site. Experimental results have shown that in all cases where doping has been achieved, dopants have either depressed T_c or had no effect on it. Where there was no effect, there is a strong suspicion that the dopant does not incorporate into the MgB_2 lattice. The case of Al has already been discussed. Felner[54] found that Be has no effect on T_c as a dopant in MgB_2, indicating that it does not incorporate into the lattice. Stoichiometric BeB_2 is not a

superconductor. Li in the magnesium site causes a shrinkage in the *a*, but not the *c*, parameter. It also decreases the superconductivity, which disappears when half the Mg atoms are replaced by Li atoms.[55] High critical current densities are still compatible with moderate levels of Ti doping,[56] and it is suspected that this dopant creates secondary phases that improve flux pinning. Kazakov *et al.*[57] studied the effects of doping with Zn and Cu. It was only possible to dope Zn into Mg-deficient MgB_2. Zn reduced both the *a* and the *c* lattice parameters and caused small reductions in T_c. Cu formed multiphase samples and apparently could not be incorporated into the lattice. Mn in the Mg site reduces the *c* lattice parameter, but not the *a* parameter, and causes steep decreases in the critical temperature, steeper than any other known dopant.[58] This is probably due to the magnetic nature of the Mn ion. Negative effects on T_c of nonstoichiometry[59] and of atomic disorder induced by neutron irradiation[60] have also been reported.

2.2 Fullerene superconductors

Organic compounds that are superconducting at very low temperatures have been well known for some time. Undoped fullerenes ('Buckeyballs') are pure carbon, with the atoms arranged in a shape resembling the geodesic domes popularised by Buckminster Fuller, as shown in Fig. 2. The crystals can be grown from vapour phase in a stream of hydrogen.[61] In their pure state these molecules are insulating, but can be doped with electrons or holes to become conducting or superconducting at low enough temperatures. In 1991, a record T_c of 18 K was announced for C_{60} crystals that were doped with potassium.[62] Doping with other alkali metals can give even higher T_c values, for instance 30 K for Rb_3C_{60}. The properties of the various compounds of this class are discussed in Lu *et al.*[63] and in Hirosawa *et al.*[64] The superconductivity of the alkali-doped fullerenes is bulk,[65] type II,[66] and generally well explained within the BCS model for low temperature superconductors, as discussed in the theory section. These compounds show a carbon isotope effect, as is expected.[67]

The fullerenes moved well into the high temperature superconductor range in 2000, when Schön *et al.*[1] were able to demonstrate superconductivity at 52 K in hole-doped

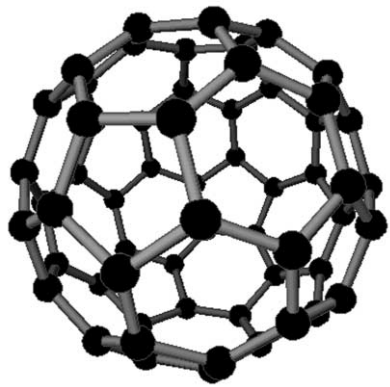

Fig. 2 Structure of C_{60} fullerene.

C_{60}. It is very difficult to add holes to C_{60} by chemical doping, so they were only able to achieve this remarkable result by incorporating C_{60} crystals into a FET device. They evaporated gold source and drain electrodes onto the crystals, then grew an Al_2O_3 dielectric layer with a gate electrode on top. Applying a positive (negative) voltage to the gate electrode induces electrons (holes) to collect in the surface layer of the C_{60} crystal, effectively doping the material. T_c depends on the charge density, with electron doping far less effective than hole doping, because the hole–phonon coupling is stronger, as indicated by resistivity measurements. The maximum T_c occurs at a doping of 3 holes per molecule.

They reported a further increase in T_c to 117 K the following year.[68] In this case the team used the same methods, but expanded the C_{60} crystal lattice by intercalating inert $CHCl_3$ and $CHBr_3$ molecules, resulting in a hexagonal crystal structure. One explanation[69] is that this worked to increase T_c (in accordance with BCS theory) because it increases the density of states available for pairing and thus the charge–phonon pairing λ. Modification of the electron–electron interaction is another possibility.[70]

2.3 The rutheno-cuprates

Magnetism and superconductivity represent two separate ordered states that materials can condense into at low temperature. These states are generally mutually exclusive. With only a 1% level of magnetic impurities, the local magnetic moments break up spin-singlet Cooper pairs and thus suppress the superconductivity. However, magnetic low temperature superconductors, such as RRh_4B_4, RMo_6S_8 and RNi_2B_2C, with R a rare earth element, have been known for some time. These families are all intermetallic, and both superconductivity and anti-ferromagnetic order can coexist, but with T_N, the Néel temperature, much less than T_c. In all these cases, the magnetic ions occupy a specific crystallographic site that is well isolated from the conductive path. This situation was also not unknown in high temperature copper oxide perovskite superconductors, provided that the magnetic ions are well isolated from the Cu–O planes that carry the supercurrents, but with $T_N << T_c$. One such example is $RBa_2Cu_3O_7$ (RBCO) with $T_c \sim 92$ K and $T_N = 2.2$ K, at most (for R = Gd).

The earliest rutheno-cuprate compounds $RuSr_2LnCu_2O_8$ (Ru-1212), with Ln = Sm, Eu or Gd, and $RuSr_2(Ln_{1+x}Ce_{1-x})Cu_2O_{10}$ (Ru-1222) were first grown,[71] although not as pure phases, and recognised as superconductors in 1995. In 1997 Felner *et al.*[72] discovered a related superconductor, $R_{1.4}Ce_{0.6}RuSr_2Cu_2O_{10-\delta}$ (R = Eu or Gd), which they named RCeRuSCO. The RCeRuSCO compounds were unique because they were both magnetic and superconducting, with $T_N >> T_c$. These compounds and others that also have $T_{Curie} >> T_c$ have been called *superconducting ferromagnets* to distinguish them from the earlier *ferromagnetic superconductors*. Work on the rutheno-cuprates has expanded over the past 3 years, with great interest in the light they throw on the nature of superconductivity.

RCeRuSCO or Ru-2122. These rutheno-cuprate compounds were first reported as both superconducting and weakly ferromagnetic[72] in 1997. They have the formula $R_{2-x}Ce_xRuSr_2Cu_2O_{10-\delta}$ where R = Gd, Eu, Sm. Table 1 shows representative Néel and superconducting transition temperatures. Detailed studies of the structure have been

Table 1 Main characteristics of the rutheno-cuprate families

Overview of rutheno-cuprate families of superconducting ferromagnets

Family	T_{Curie}/K	T_c/K	Notable features
*R*CeRuSCO or Ru-2212 ($R_{2-x}Ce_xRuSr_2Cu_2O_{10-\delta}$ with *R* a rare earth)	AFM ordering of Ru layers $T_{Curie} = T_N$ values for $x = 0.6$ [73]		Repeating RuO_6, CuO_2 and $R_{2-x}Ce_xO_2$ layers space group *I*4/*mmm* spontaneous vortex state
R = Gd [73]	180	42	
R = Eu [73]	122	32	
R = Sm [73]	220	28	
Ru-1212 ($RuSr_2RCu_2O_8$, with *R* a rare earth)	Magnetic ordering still under dispute, possibly AFM ordering in *c* direction at low fields, FM at high fields [74]		Layered structure: CuO_2, *R*, CuO_2, SrO_2, RuO_2, SrO_2 space group *P*4/*mmm* possible spontaneous vortex state at low fields [74]
R = Gd [75,76,77]	132	~45 T_d ~30 K	Gd and Ru couple across CuO_2 planes
R = Eu [74]	132	32, T_d ~10 K	
R = Sm [78]	146	12	
R = Y [79]	150	45	
R = Pr [80]	Not a superconductor		
The O_6 Ruthenates [81]	FM in *a*–*b* plane, AFM in adjacent sheets in *c* direction,		Alternating layers of (Sr,Ba)O and (Y,Ho)RuO_4
($(Sr,Ba)_2(Y,Ho)Ru_{1-x}Cu_xO_6$)	values for $Sr_2YRu_{1-x}Cu_xO_6$		no copper oxide planes
	86	45, T_d = ~30 K	

made by Kuz'micheva *et al.*[82] and by Knee *et al.*[83] Some related compounds, *M*-2212 are also superconducting, but X-ray absorption spectroscopy has revealed that this is only true where *M* is pentavalent, *i.e.*, for Ta, Nb and Ru.[84]

The structure of the Ru-2212 perovskite compounds is tetragonal (space group *I*4/*mmm*). a = 3.846 (3.844) Å and c = 29.50 (28.62) Å for EuCeRuSCO (GdCeRuSCO). The Ru-2122 structure can be derived from the YBCO structure by replacing the Y layer by fluorite type $R_{2-x}Ce_xO_2$ layers and replacing the Cu–O chains by RuO_6. The repeating layers are thus RuO_6, CuO_2 and $R_{2-x}Ce_xO_2$. The non-stoichiometry δ is large,[83] up to 0.22. The hole doping of the superconductor is controlled by the *R*/Ce ratio.[85] No variations in the lattice parameters are observed in XRD at T_c or T_M.[86]

The same grains in *R*CeRuSCO are both superconducting and magnetic. Scanning tunneling microscopy has shown a superconducting gap for the whole structure.[72] There is general agreement that the superconductivity is due to holes in the copper oxide planes and that the magnetism is due to the Ru sublattice. This is supported by magnetic susceptibility and Mössbauer spectroscopy measurements.[72] Iron doping (x = 0.13 and 0.25) into the Ru site of Ru-2212 suppresses the superconductivity and diminishes the weak ferromagnetic properties,[87,88] indicating that these properties are due to the Ru site.

*R*CeRuSCO compounds are characterised by a spontaneous vortex state.[89,90] There is a peculiarity in that the temperature for the onset of the diamagnetism T_d (~20 K for EuCeRuSCO, x = 0.6) is considerably lower than the superconducting transition temperature T_c. Between these two temperatures there are always magnetic flux lines

present, even at zero external field (the spontaneous vortex phase). Below T_d flux is expelled from some magnetic domains. The spontaneous vortex state has been visualised by magneto-optical imaging.[91] Chen *et al*.,[92] however, attribute the absence of the bulk Meissner effect to the presence of an impurity phase.

Ru-1212. Ru-1212 ($RuSr_2RCu_2O_8$, with R a rare earth) was first reported[93] in 1997 as ferromagnetic for R = Gd. This compound was identified as both ferromagnetic and superconducting at the 1998 Applied Superconductivity Confererence.[94] Single crystals of Ru-1212 have been grown using the self-flux method,[95] while thin films have been made by pulsed laser deposition.[96] Table 1 contains details on the individual compounds.

There are some discrepancies in T_c values in the literature, depending on whether the onset is defined by a decrease in the ac susceptibility. It is argued that the decrease marks the appearance of the superconductivity, with the bulk Meissner effect suppressed down to a lower temperature T_d, possibly due to a spontaneous vortex phase as in *R*CeRuSCO.[74] Chu *et al.*[97] believe that there is evidence for a novel superconducting state in $RuSr_2GdCu_2O_8$ that is characterised by the absence of a bulk Meissner effect, negligible superconducting condensation energy, and an unusually large penetration depth. There is experimental evidence[98] for the absence of the bulk Meissner effect down to 2 K and 0.2 Oe, but this has been disputed by Bernhard *et al*.[99] Experimental work[100] also suggests a 30–50 μm effective penetration depth.

Ru-1212 is a triple perovskite,[101] with the structure closely resembling that of other 1212 copper oxide high temperature superconductors, as shown in Fig. 3. Two CuO_2

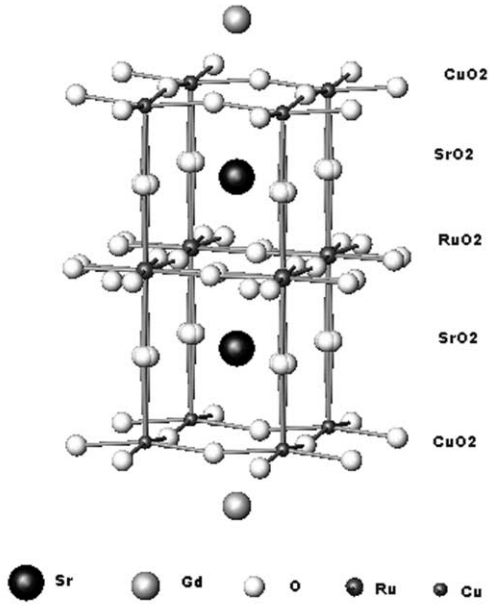

Fig. 3 Structure of $RuSr_2GdCu_2O_8$, a Ru-1212 compound.

planes have *R* ions between them and are separated from the magnetic RuO_2 layers by SrO_2 layers. The space group is *P4/mmm*, and the unit cell is tetragonal with (for *R* = Gd) a = 3.84 Å and c = 11.6 Å. Unlike *R*CeRuSCO, there is no evidence for oxygen non-stoichiometry in this material.[101–103] However, some workers report that excess oxygen from oxygen treatment produces beneficial effects such as increasing T_c.[82,104,105]

Tin doping into the Ru site[106–108] in $RuSr_2GdCu_2O_8$ suppresses the ferromagnetic order, decreasing the Curie temperature and increasing T_c to 78 K for x = 0.4. V enhances both the ferromagnetism and the superconductivity, provided that $x < 0.2$, while Ti and Nb weaken both.[107,109] Nb has the same effect[110] in $RuSr_2EuCu_2O_8$. Zn doping also suppresses superconductivity[76] as in other high-T_c cuprates, as does Ta doping.[92,104] Klamut *et al.*[105,111] investigated the effects of replacing some of the Ru with Cu and found that it was possible to raise T_c to 72 K by adjusting the Ru/Cu ratio.

Heat transport and heat capacity measurements indicate bulk superconductivity. They show the typical behaviour of a short-coherence length, underdoped high-T_c cuprate, with the transport properties dominated by the CuO_2 layers.[76] This view is supported by infrared conductivity evidence.[112] Blackstead *et al.*,[113] however, suggest that magnetic ordering of the Cu ions implies that the superconductivity takes place in the SrO_2 layers.

NMR experiments[114] have suggested that it is the Ru^{5+} ions that are responsible for the ferromagnetism in Ru-1212 while the Cu ions are nonmagnetic. Some workers[115–117] present evidence for a mixed Ru^{4+}, Ru^{5+} valence from magnetisation and magnetic resonance measurements. There is no evidence of any effect on the magnetic properties due to the onset of superconductivity. Magnetic resonance experiments by Srikanth *et al.*[118] give evidence for magnetic anisotropy in the normal state.

Muon spin relaxation measurements[77] show a spatially homogeneous magnetic order, as do magnetic resonance experiments.[119] There is still no consensus on the precise nature of the magnetic order in these compounds, in terms of whether it is ferromagnetic or antiferromagnetic in some or all directions, how the Ru moments are aligned, and whether the order varies depending on the external field. A full discussion of these issues can be found in Williams and Krämer[74] and in Tokunaga *et al.*[79]

The magnetic resonance experiments of Fainstein *et al.*[119] have revealed coupling between Ru and Gd ions in the Gd compound, even though the conduction electrons are between them in the CuO_2 layer. This possibly accounts for the relatively low T_c. Magnetisation, magnetoresistance and NMR experiments have in fact confirmed a small interaction between the Ru moments and the conduction electrons,[117,120] and this is consistent with theoretical calculations..[121–123] There is also a considerable body of theoretical work that investigates the general mechanisms responsible for the coexistence of superconductivity and magnetism in Ru-1212.[124–129]

$(Sr,Ba)_2(Y,Ho)Ru_{1-x}Cu_xO_6$, the O_6 ruthenates. $Sr_2YRu_{1-x}Cu_xO_6$ and $Ba_2YRu_{1-x}Cu_xO_6$, compounds from this family were first reported to be superconducting in 1997 by Wu *et al.*[130,131] $Sr_2HoRu_{1-x}Cu_xO_6$ is also superconducting.[132] The O_6 ruthenates combine antiferromagnetic order with superconductivity. They are of particular interest because there are no copper oxide planes,[133] with Cu doping into Ru sites, and because closely related compounds with the same structure, such as Ba_2GdRu_{1-x}-

Cu_xO_6, are not superconducting. In $Sr_2YRu_{1-x}Cu_xO_6$, $T_c \approx 45$ K with Cu ions ordered at 86 K and Ru ions at 23 K.[134] In the Ho compounds there is an additional magnetic ordering at 15 K, representing a ferromagnetic transition.[135] The crystal structure consists of alternating layers of (Sr,Ba)O and $YRuO_4$, as shown in Fig. 4. There is evidence that superconductivity takes place in the p- type (Sr,Ba)O layers.[136]

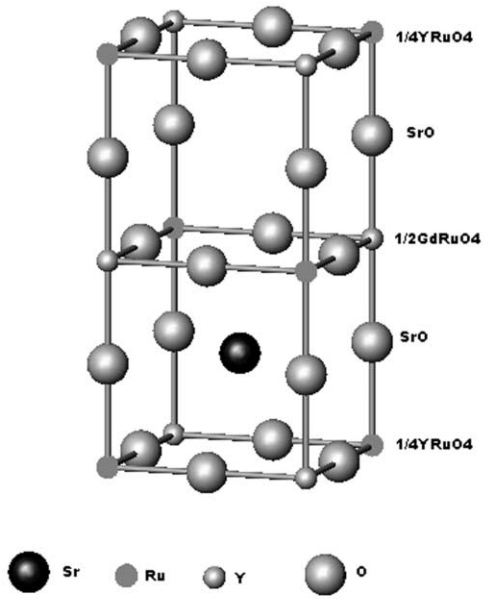

Fig. 4 Structure of the O_6 ruthenate $Sr_2YRu_{1-x}Cu_xO_6$. Note the absence of CuO_2 planes.

Mössbauer effect measurements have confirmed that superconductivity and homogeneous magnetic order coexist.[137] The Ru moments order ferromagnetically in the *a–b* plane, with adjacent sheets in the *c* direction ordered antiferromagnetically.[138] Harshman *et al.*[139] identified a spin glass state at 29.3 K on the basis of muon spin resonance and electron spin resonance measurements.

Blackstead *et al.*[134] believe that superconductivity in these compounds needs to be explained by their oxygen model, which locates the superconductivity in the (Sr, Ba)O planes and only allows crystal-field split rare earth ions to coexist with Cooper pairs. $Ba_2GdRu_{1-x}Cu_xO_6$ is not superconducting because L=0 Gd is not crystal field split. Wu *et al.*[131,135] explain the superconductivity by a double exchange interaction that involves Ru^{5+} ions.

2.4 MBE grown new copper oxide high temperature superconductors

A group of Japanese researchers[140] has pioneered the growth of thin films of new and existing high-temperature superconductors by molecular beam epitaxy (MBE). While the use of an appropriately lattice-matched substrate and proper growing temperature

is important for achieving success, MBE substantially eliminates contamination and gives control over growth on an atomic mono-layer level. The first new superconductor was $Ba_2CuO_{4-\delta}$. Ba_2CuO_{3+q} was first grown on a $SrTiO_3$ substrate, then converted to $Ba_2CuO_{4-\delta}$ by oxidising in ozone. The compound has a K_2NiF_4 based structure with $T_{c(onset)} \sim 90$ K. The sister compound $Sr_2CuO_{4-\delta}$ has also been grown.[141] Two researchers in the group, Karimoto and Naito,[142,143] have also succeeded in growing $PbSr_2CuO_{5+\delta}$ (Pb-1201) on a variety of substrates, using substrate temperatures below 600 °C. T_c is only of the order of 40 K, but Karimoto and Naito believe that they will also be able to grow related higher T_c compounds by the same technique.

3 Theory of superconductivity in high-temperature superconducting cuprates and other materials

Over the last few years the experimental and theoretical study of the high temperature superconducting (HTSC) cuprates remains one of the leading issues in the physics of condensed matter. However, in spite of great efforts there is no clear consensus in the superconductivity community on the nature of this phenomenon.[144] In our opinion, the development of the theory of high-temperature superconducting cuprates could well be described by the statement-question of Batlogg from Bell Labs in his closing remarks to the M2S-HTSC-VI Conference in Houston, February 2000: ". . .*more data – less clarity*. . .!?" This is mainly due to the well-known complexity of copper oxides and, as a consequence, due to the difficulty in preparation of standard perfect samples, particularly single crystals having a certain standard of doping degree, homogeneity, and superconducting properties. Rather large scattering in these parameters has led to a huge variety of experimental results overshadowing the real picture. On the other hand, the complexity is also associated with exotic properties of the cuprates in their normal (non-superconducting) state.[145,146] Without understanding these properties it is hardly possible to elucidate the microscopic mechanism of HTSC. In this respect, the phenomenon known as the pseudogap state looks particularly intriguing and is currently under intensive research.[145–147]

Furthermore, the questions about mechanisms of superconductivity have recently experienced a great new boost after two new exciting discoveries in 2001: (i) in January the superconductivity community was shaken by the unexpected discovery of the new 40 K superconductor MgB_2. In spite of its apparent structural simplicity compared to the cuprates, it seems that MgB_2 also has the complex nature of superconductivity, as shown, for example, in reduced total isotope effect experiments.[148] (ii) In September the critical temperature T_c of a special form of crystalline carbon C_{60} hit an astounding 117 K.[149]

In this section we concentrate on HTSC cuprates, mainly reviewing issues associated with the phenomenon called the pseudogap, which has been the hottest topic related to the theory of superconductivity in the cuprates within the last three years. However, we also highlight the latest developments in determining the mechanisms of superconductivity in the newly discovered *high temperature* superconductors MgB_2 and the doped fullerenes.

3.1 High-temperature superconducting cuprates

Fig. 5 shows a typical version of the generic phase diagram of the high-T_c superconducting cuprates. Because of its frequent appearance in numerous presentations during the M2S-HTSC-VI 2000 Conference in Houston, Laughlin from Stanford University even suggested that the participants call this phase diagram the logo of the conference. The phase diagram exhibits a number of phases and regions with different physical properties depending on the concentration of charge carriers, mainly holes in conducting CuO_2 planes. All the known cuprates can be considered as insulating antiferromagnets (AF).[150,151] On increasing the hole concentration, the Néel temperature T_N rapidly drops to zero and an increase in conductivity results in an insulator–metal transition. As the level of the hole doping is increased, the system becomes superconducting. The T_c of this superconductor increases up to a maximum at a certain optimal concentration p_0 of the charge carriers and then decreases until its total disappearance. In this entirely overdoped state, however, the system preserves its metallic properties. At $p > p_0$ the metallic properties are fairly conventional, *i.e.*, described within the Fermi-liquid approach. Whereas at $p < p_0$, the system is a "bad" metal and cannot be described by the Fermi-liquid theory.[152,153]

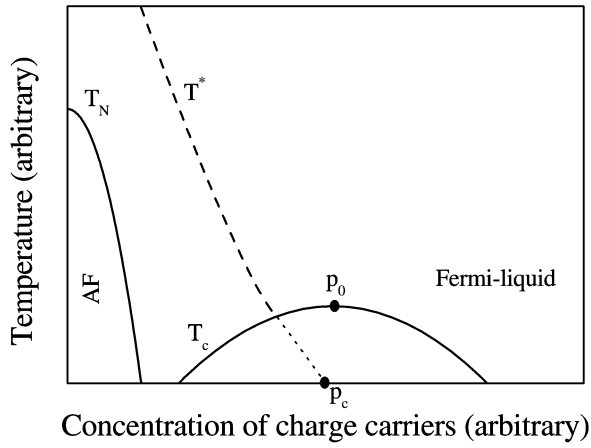

Fig. 5 Schematic generic phase diagram of the high-T_c superconducting cuprates.

In the region where $p < p_0$ and $T < T^*$, where T^* is the temperature at which the pseudogap appears, the variation of the resistivity ρ as a function of temperature is not linear, having a downwards curvature above T_c, in contrast to the optimally doped state showing a linear temperature dependence (see, for example, refs. 154–156] and references therein). T^* decreases from temperatures above T_N at low doping levels and can either (i) merge with the T_c line or (ii) become zero at some critical concentration of the charge carriers,[145,154,156] as shown in Fig. 5. However, generally, as has been shown by numerous different experiments[154] including measurements of susceptibility, specific heat, angle resolved photoemission spectroscopy (ARPES), NMR relaxation time, and resistivity, the pseudogap vanishes at some critical hole

concentration p_c which enables the interpretation of this critical value as some sort of "quantum" critical point in Tallon *et al.*[157] The first possibility, merger with the T_c line, is usually associated with the superconducting nature of the pseudogap: uncorrelated (incoherent) Cooper pairs already formed above the critical temperature[155,158–165] consecutively achieve phase coherence at $T \geq T_c$. In the last few years the second possibility, disappearance at a critical concentration of charge carriers, has attracted more interest and has led to several scenarios advocating a correlation in the particle–hole channel, such as the antiferromagnetic correlation,[167–169] charge stripes,[156,170,171] and quantum criticality.[172]

As mentioned above, the non-superconducting view of the pseudogap may have appeared to be dominant during the past few years, but it is far too early to give up on incoherent pairing[173] as being responsible for the pseodogap anomalies. In a recent work[174] it was found that the Nernst effect in $La_{2-x}Sr_xCuO_4$ (LSCO) above T_c is too large to be described by the usual electronic mechanism, and the most likely explanation is moving vortices. Although LSCO superconductor is quite different from other high-T_c cuprate superconductors, such as YBCO and BSCCO, there were some indications that YBCO behaves similarly. This explanation of the effect suggests that in the state where the pseudogap exists there are sufficiently large regions to provide accommodation for the vortices and, therefore, be considered truly superconducting. These experimental results were immediately analyzed theoretically,[175] and the superconducting pseudogap phase with vortices was qualitatively explained on the basis of a resonant tunnelling connection of the electrons between CuO_2 layers through localized states at the oxygen atoms in the intermediate layers.[176]

Numerous experimental results show that the conductivity measured at high temperatures above T_c always falls below the theoretical prediction.[155,177] To explain this behavior a two-channel model for the conductivity of underdoped YBCO was suggested in Leridon *et al.*[155] One channel is the single-particle excitation dominating in optimally doped material (having a linear resistivity as a function of temperature), the other gives a contribution merging with the 3D Aslamazov–Larkin fluctuation conductivity at low temperature and obeying a power law at high temperatures. The conductivity of the latter channel depends on two superconducting parameters, namely T_c and the zero temperature coherence length ξ_0. Thus, the model is consistent with the coexistence of incoherent pairing and single-particle excitations. Such a "soup" (coexistence) of fermions and pairs of fermions is discussed, for example, in Chen *et al.*[163,164]

There is a trend in the majority of most recent papers on the topic to favour another point of view: the "non-superconducting" nature of the pseudogap. Here we try to highlight only some of the most recent developments in this stream. However, we address readers to recent topical review papers[145,154] which can provide a wider scope on this issue than the brief outline given in this review.

Upon discussing tunneling spectroscopy experiments in the high-T_c cuprates, one always asks about the surface quality of the samples being investigated. Therefore, a recent *intrinsic* tunneling spectroscopy study in BSCCO materials is of particular interest.[178,179] The experiments were done in high magnetic fields used for a direct test of superconducting features in the quasiparticle density of states. It was possible to distinguish with great clarity two coexisting gaps: (i) the superconducting gap, which closes as the applied magnetic field approaches the second critical field, and

(ii) the *c*-axis pseudogap, which does not change either with the applied field or with temperature. The different field dependences, together with the observed different temperature dependences of the two gaps, enabled the authors to make a claim against the superconducting origin of the pseudogap.

The existence of the pseudogap can be observed in kinetic properties (such as the Knight shift and NMR relaxation time) of the cuprates in the normal state. As mentioned above, the pseudogap is associated with a change in the standard (for optimally doped composition) linear temperature dependence of the resistivity in the region $T < T^*$ for underdoped samples.[145] The temperature dependent NMR spin lattice relaxation rate of ^{63}Cu for near optimally doped YBCO, near and above T_c, was found to be insensitive to magnetic fields of up to 14.8 T.[180] In a slightly *overdoped* superconductor, the Knight shift and the nuclear spin–lattice relaxation rate were found to be strongly dependent on magnetic field.[181,182] This pseudogap behavior, *i.e.*, the reductions in the Knight shift and the relaxation time above T_c from the values expected for the normal state at high temperatures, is strongly field dependent and follows a scaling relation. This scaling was shown to be consistent with the effects of the Cooper pair density fluctuations. In the *underdoped* regime no field effect was seen up to 23.2 T . The results in Zheng *et al.*[181,182] can point to the disappearance of the non-superconducting pseudogap (independent of magnetic field) at some smaller concentration of charge carriers. It should, however, be noted that the above mentioned experiments[180–182] are at odds with other studies showing a clear difference in the relaxation time in both the absence and the presence of a magnetic field up to 27.3 T parallel to the *c*-axis.[183] The magnetic field independent behavior would be a strong argument in favor of the non-superconducting nature of the pseudogap, but we believe that further study is necessary to resolve the experimental controversy. Recently, a systematic study of interlayer tunneling resistivity in high fields up to 60 T suggested some possible models for cuprates having various doping levels.[184]

Experiments measuring optical conductivity clearly reveal the pseudogap manifestation in the direction of the electric field vector along the conducting CuO_2 layers, as well as in the orthogonal direction along the tetragonal *c*-axis.[152,185,186] The characteristic features of the optical reflectivity measurements are a narrow Drude peak in a low frequency range and reflectivity depression at higher frequencies. The latter feature is considered a hallmark of the pseudogap state. Although the optical data merely show the (co-)existence and the energy ranges for both features, nevertheless, they allow the claim that the superconducting gap and the pseudogap are not the same due to, for example, the fact reported in Singley *et al.*[186] that the pseudogap and superconducting energy states differ by more than one order of magnitude.

Measurements of transport properties in underdoped YBCO thin films in fields up to 50 T have recently allowed an unambiguous interpretation of the pseudogap as the spin gap in spin ladders within the framework of the one-dimensional hole-rich *stripe* transport model.[156] This model arose due to growing evidence (see references in Moshchalkov *et al.*[156]) that the CuO_2 planes are not doped homogeneously, but instead, hole-rich one-dimensional (1D) features (stripes) are formed. This intercalation of antiferromagnetic insulating regions and metallic hole-rich stripes forms below T^*, where the pseudogap develops. Since mobile carriers in the case of underdoped high-T_c cuprates are expected to be expelled from the surrounding Mott-insulator phase into the stripes, the latter then provide the lowest resistance paths.

Therefore, the transport properties should be very sensitive to stripe formation which is used in ref. 156 to carry out the study.

Very pronounced effects associated not only with the pseudogap, but also with manifestations of "conventional" superconductivity can be obtained with the help of ARPES. This technique has been rapidly developing over the past decade with improvements in both energy and momentum resolutions. A review[187] of ARPES data on the cuprates ranging from insulator to overdoped systems discusses some recent experimental and theoretical efforts to understand the superconducting state and the pseudogap phenomenon. The effects of charge stripes on ARPES spectra are also reviewed. Quantitatively, ARPES experiments give direct information on spectral properties of single-particle excitations in the system measured.[145] Typical ARPES data[188] show how the superconducting gap, existing below T_c and consistent with the d-pairing symmetry at low temperatures,[189] closes at $T = T_c$ for an optimally doped system. For underdoped systems, on the other hand, the gap gradually transforms into the pseudogap at $T > T_c$.[188] This transformation is often considered as evidence for the superconducting nature of the pseudogap, but discussion on this issue is far from being closed.[145]

Note that the ARPES data are practically the only source of information on the Fermi surface (FS) of the cuprates.[190] Without going into detail, the structure of the FS and the spectrum of elementary excitations in CuO_2 planes obtained in ARPES experiments can be fairly well described by the strong coupling model.[145] However, the situation with regard to the true topology and character of the normal state FS of, for example, the Bi-2212 system as seen by photoemission spectroscopy is nowadays the matter of intensive debate:[145,191–195] ARPES data have been interpreted in terms of a FS with missing segments and an extra set of one-dimensional states, as well as an electron-like FS centered around the Γ point, a hole-like FS with the form of rounded tubes centered on the corners of the Brillouin zone, and even both electron-like and hole-like FS pieces observed simply depending on the photon energy used in the ARPES experiments.[191–195]

Another intense debate over pairing symmetry in the cuprates was resolved to a certain extent, with the help of the development of phase-sensitive symmetry tests,[189] in favor of a predominately anisotropic d-wave orbital order parameter symmetry for the *hole-doped* high-T_c cuprates. However, until recently the symmetry of the superconducting pair state in the *electron-doped* cuprates remained controversial. A series of phase-sensitive experiments has been presented as evidence for d-wave pairing in electron-doped superconductors.[196] This evidence was obtained by observing the half-flux quantum effect, using a scanning SQUID microscope.

The majority of the theoretical work on high-T_c cuprates is associated with different modifications of the Hubbard model, which mainly deals with a strong Coulomb repulsion from a single center. The two most elaborated models of the high-T_c cuprates can be found in Anderson.[197,198] Both approaches are based on the model of the so-called resonance valence bonding,[199] describing a spin liquid of singlet electron pairs. However, ever since they appeared both models have been criticized by experimentalists.[200–203] Generally, the review, ref. 144, on the nature of high-T_c cuprates emphasizes that the normal state of these systems is hardly different from that of the "conventional" metals. It also concludes that with the help of the electron–phonon interaction (EPI) it is possible to explain many low-energy

relaxation processes in high-T_c cuprate systems including the high critical temperature values. However, it is emphasised that the EPI alone is not able to describe many other different features such as anisotropic *d*-pairing. That is why one has to take into account the strong Coulomb repulsion. The current state of the existing models and supporting experimental observations is also considered in ref. 144.

3.2 MgB_2 superconductor

The avalanche of publications on superconducting MgB_2 in 2001 also contains some early attempts to explain the superconductivity mechanism in this material.[43,148,204–219] While the high transition temperature might imply exotic coupling mechanisms, the boron isotope effect in MgB_2 is consistent with the material being a phonon-mediated Bardeen–Cooper–Schriefer (BCS) superconductor.[204] This conclusion was made in ref. 204 after finding a 1.0 K shift in T_c between $Mg^{11}B_2$ and $Mg^{10}B_2$ systems upon measurements of both temperature dependent magnetization and specific heat. However, a much smaller but measurable Mg isotope effect was also reported[148] making the total reduced isotope-effect coefficient 0.32, which is much lower than the value expected for a typical BSC superconductor. This low value could be due to complex materials properties, and, as in the case of HTSC cuprates, would require both a large electron–phonon coupling constant and a repulsive electron–electron interaction that is larger than is found for most simple metals. Controversially, recent reflectance measurement analysis[205] on *c*-axis oriented thin films within the conventional electron–phonon framework implies that the EPI is very weak and insufficient to produce $T_c = 39$ K in MgB_2. A simple model was constructed with coupling to a high frequency excitation, which is consistent with both the low frequency optical data and the high value of T_c.

On the theoretical side, it seems that the majority of the theorists supports the BSC mechanism, *i.e.*, an electron–phonon driven s-wave mechanism of the superconductivity in MgB_2, having, however, some new features due to its high T_c value and fundamental differences from the cuprates.[207–209] On the other hand, there are a few other attempts to provide the same physical mechanism for both MgB_2 and HTSC cuprates.[210,211] The underlying idea is to use the theory of hole superconductivity which explains high temperature superconductivity in cuprates as driven by pairing of hole carriers in oxygen p-orbitals in the highly negatively charged Cu–O planes. The pairing mechanism is hole undressing, and is Coulomb-interaction driven. In MgB_2 the planes of B atoms are proposed to be akin to the Cu–O planes in the cuprates, and the high temperature superconductivity in MgB_2 arises similarly from undressing of hole carriers in the planar boron $p_{x,y}$ orbitals in the negatively charged B-planes. Within the mechanism proposed,[210,211] doping MgB_2 with electrons and with holes should mirror the behavior of underdoped and overdoped high-T_c cuprates, respectively. Furthermore, there are a variety of other mechanisms proposed that might allow the claim that the same mechanism is responsible for superconductivity not only in the HTSC cuprates and MgB_2,[212,213] but also in conventional superconductors, and indeed in all other superconductors.[214] In the latter work,[214] one can also find a brief review of the experimental situation with respect to MgB_2 superconductors from the point of view of the hole superconductivity mechanism (see also ref. 210 and 211).

A number of measurements have been made with a view to determining the superconducting energy gap. Although the results seem to indicate an isotropic order parameter, they were inconsistent with a single, isotropic gap. The presence of two gap structures has been proposed.[215–218] Both gaps were found to close at the bulk transition temperature. Adding to the controversy, the existence of two superconducting gaps in MgB_2 was predicted theoretically in Liu *et al*.[209] The electronic structure of MgB_2 is quite complex; in particular, the FS presents the coexistence of both quasi-2D covalent cylindrical sheets and a 3D metallic-type interlayer conducting network,[219] which raises the possibility of having, in the clean limit, two distinct gaps both closing at the same temperature. Thus, these experimental observations and the preceding theoretical prediction indicate that MgB_2 is the precursor of a new class of multiple-gap superconductors.[215–218]

3.3 Fullerene superconductors

Recent reports[1,149] drastically alter the perception that the planar cuprates are the only route to high temperature superconductivity. Another exotic class of superconductors, fullerenes, has entered the high-T_c superconductivity "club". Although crystalline C_{60} is normally an insulator it was shown[62] in 1991 that electron doped fullerenes are superconducting at 18 K. Recently, the T_c in C_{60} was raised to 52 K by field-effect hole doping, suggesting that the T_c could be further raised by increasing the intermolecular distance, a quantity that was found to be almost linearly related to T_c.[1] The results in ref. [149] confirm these expectations. C_{60} single crystals were intercalated with $CHCl_3$ and $CHBr_3$ in order to expand the lattice. A high density of electrons and holes was induced by gate doping in a field-effect transistor geometry. At low temperatures, the material turns superconducting with a T_c of up to 117 K, which was reported[149] in hole-doped $C_{60}/CHBr_3$.

It is widely believed that hole-doped C_{60} follows the standard model of superconductivity in which phonons provide the source of attraction between carriers for pair formation and concomitant zero resistance.[70] In fullerenes, high-energy intramolecular phonons are available to mediate the pairing. As the distance between molecules increases, the overlap of electronic wave functions decreases. As a result, the electronic bands narrow and the electronic density of states at the Fermi surface increases. These effects, supplemented by a substantial electron–phonon coupling, appear to determine to a large extent the high value of T_c.[70] Smaller fullerenes are anticipated to have even higher T_c values than C_{60} if the right charge density can be induced by using the field-effect doping method.[68]

4 Vortex matter

4.1 High temperature superconductor vortices

Most high temperature superconductors (HTS) are typical type-II superconductors. Their behavior is dominated by the presence of vortices in the mixed state. Because of high transition temperatures, small coherence lengths, large penetration depths and

strong anisotropy, high temperature superconductors demonstrate rich and complicated vortex behavior, which has attracted intensive studies on this unique phase of matter in recent years.

Visualization of vortices and their movement. A modified Bitter technique[220] has been employed to directly observe the shape, form and distribution of vortices and vortex movement in HTS samples using an *in situ* nano-coating technique. Vortex movement has been identified while the transport current was applied in Bi-2212 single crystals. Recent observation of vortices in Bi-2223/Ag tapes using the same technique shows that the correlation between microstructure and vortex distribution provides clear evidence on whether introduced defects are effective pinning centres. Fig. 6 is a comparison of images taken from Bi-2223/Ag tapes, one (left) being doped with uranium and irradiated by thermal neutrons and the other one (right) being the normal tape. It is clear that the tracks induced by the U/n technique in the irradiated tape resulted in more trapped vortices than in the un-irradiated tape.

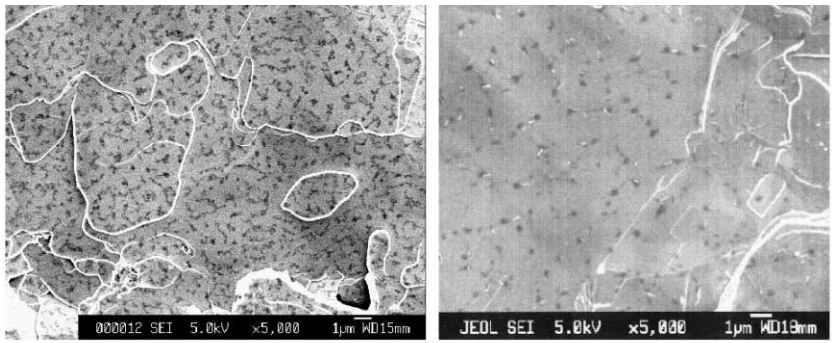

Fig. 6 By using the Bitter decoration technique, vortex patterns in Uranium doped Bi-2223 tape (left) and undoped tape (right) are visualised at 28 K and a magnetic field of 7.5 mT.

Images of individual vortices trapped along columnar defects in Bi-2212 thin films have been obtained[221] with the help of a 1 MV field-emission electron microscope. For the films investigated, it was found that the vortex lines are trapped and oriented along tilted columnar defects at rather high temperatures, irrespective of the orientation of the applied magnetic field. It was, however, observed, that at lower temperatures vortex penetration always takes place perpendicular to the film plane, suggesting that bulk ("background") pinning in the material dominates.

Vortex pinning by columnar defects. Because of the cylindrical structure of the flux lines, irradiation of samples with heavy ions, so as to create cylindrical damage tracks throughout the sample, provides one way of artificially introducing anisotropic pinning. Although this method has been used for years, more detailed studies have been performed on this topic in recent years. Lee *et al.*[222] used muon spin rotation and small angle neutron scattering technique to investigate the properties of BSCCO single crystals irradiated with fast heavy ions, providing substantial evidence that even below the matching field, the positions of the vortices are not random in a plane perpendicular to the tracks. The crossover to a glassy vortex arrangement is moved to higher

fields than is the case in the pristine material. The presence of the columnar defects also strongly suppresses thermal fluctuations of the vortices.

Several groups have studied the phase diagram of untwinned YBCO crystals with dilute columnar defects.[223–225] Kwok *et al.*[223] found that columnar defects create a lower critical point in YBCO, separating a low field Bose glass from the high field vortex lattice. The intersection of the second order Bose glass transition line with the first order melting line at the lower critical point provides evidence for the existence of a disorder-to-order vortex transition line in the vortex solid near the lower critical point. An enhancement of the upper critical point with dilute columnar defects has also been demonstrated. The results indicate the important role of the vortex tilt modulus at high fields, giving strong support for a vortex entanglement transition near the upper critical point.

An asymmetric critical-state field profile in YBCO with columnar defects has been observed when the field is tilted away from columnar defects, with the profile depending on the field sweep direction and the misalignment of the field from the columnar defects.[226] From magneto-optical imaging performed on heavy-ion-irradiated YBCO single crystals, Morozov *et al.*[227] found that in order to depin vortices that are trapped along their entire length by columnar traps, it suffices to nucleate vortex kinks at the sample surface only; further depinning occurs by kink sliding. The vortex liquid phase has also been studied in heavy-ion-irradiated BSCCO crystals.[228]

Vortex pinning by extended defects in YBCO thin films. Much attention has recently been paid to extended defects, such as dislocations, grain boundaries, twin boundaries, surface corrugations and anti-phase boundaries. One reason for this is that extended defects may be the cause of the high critical currents observed in high temperature superconductors, while oxygen vacancies provide only weak pinning. On the other hand, extended defects may have profound effects on the phase diagram of high temperature superconductors and can thus be used to study the phase diagrams and verify the pinning models.

Dam *et al.*[229] found that both edge and screw dislocations provide the strong pinning centers needed for the high critical currents observed in YBCO thin films. However, as shown in ref. 230 high critical current densities in YBCO films seem to be mainly governed by *linear edge dislocations* since their density exceeds the density of the screw dislocations by 1–2 orders of magnitude. By studying the superconducting current density, the dynamic relaxation rate, and the pinning potential, Klaassen *et al.*[231] demonstrated that growth induced linear defects act as strong pinning centers in YBCO thin films. By measuring the dependence of the critical current density of an YBCO bicrystal film on the orientation of the magnetic field, Diaz *et al.*[232] provided evidence for strong vortex pinning by dislocations in low-angle grain boundaries. Anti-phase boundaries have also been reported to be strong pinning centers in YBCO thin films.[233]

Moreover, twin boundaries have been reported to play an important role in determining the vortex structure and flux pinning of YBCO.[234] The planar nature of the twin boundaries allows for the study of the interaction between vortices and two-dimensional defects. Anisotropic pinning behavior for flux motion parallel and perpendicular to the twin boundaries might be expected. For homogeneous twin planes, pinning against motion parallel to the boundary is not expected, but pinning by twin

boundaries occurs when the Lorentz force is directed perpendicular to them, as has been clearly demonstrated by angular dependent magnetoresistance measurements. There have also been several recent reports on the fabrication of twin-free or unidirectionally twinned YBCO thin films,[235] which allows detailed investigations on the pinning properties of twin boundaries. Although it has been reported that twin boundaries provide guided motion for flux lines moving parallel to the twin boundaries,[236] Yamasaki *et al.*[237] have pointed out that the guided motion may be caused by micro-cracks along twin boundaries, rather than by twin boundaries themselves. Therefore, in order to clarify the pinning effects of twin boundaries, further work is needed.

Peak effect, order–disorder transition. In type-II superconductors, one often observes that the critical current density increases with the applied magnetic field at fixed temperature - the peak effect (or fishtail effect). As has been pointed out by Paltiel *et al.*,[238] although several sharp features have been observed at the peak effect and various models for the peak effect suggested, there is currently no general consensus regarding the underlying mechanism. At present, the peak effect is widely attributed to the transition from a quasi-ordered Bragg glass into a disordered amorphous vortex phase.[239–242]

Transport studies by Paltiel *et al.*[238,240] suggest that the ordered Bragg glass undergoes a first order transition into an ordered solid. A detailed description of the order–disorder transition in the H-T phase diagram of 3D type-II superconductors with accounts of both pinning related and thermal fluctuations of the vortex lattice has been presented by Mikitik and Brandt.[243] It is shown that the shapes of the order-disorder transition line and the vortex lattice melting curve are determined only by the Ginzburg number, which characterizes thermal fluctuations, and by a parameter which describes the strength of the quenched disorder in the flux line lattice.

The dynamic anomalies and history effects related to the order–disorder transition have been widely reported.[238,240,244–247]

However, whether the order–disorder transition is at the peak effect or below or above it is currently controversial. Correa *et al.*[248] have argued that the peak effect has its origin in changes of the elastic equilibrium properties of the vortex structures, rather than the order–disorder transition. Furthermore, Esquinazi *et al.*[249] have suggested that the peak effect might also originate in the thermomagnetic flux-jump instability effect. The order–disorder transition and the peak effect therefore require further theoretical and experimental work to clarify the underlying physics and mechanism.

Current driven vortex lattice–dynamic phase transition. Although the static phases of vortex matter have been well understood, the dynamic phases of vortex matter driven by applied currents are still under investigation. The dynamic phase transitions of driven vortex matter have recently attracted considerable attention.[247,249–252]

Olson *et al.*[251] have shown that, at high driving currents, at least *two distinct dynamic phases* of flux flow appear depending on the vortex–vortex interaction strength. When the flux lattice is soft, the vortices flow in independently moving channels with a smectic structure. For stiff flux lattices, adjacent channels become locked together,

producing crystalline-like order in a coupled channel phase. At the crossover between these phases, the system produces a maximum amount of voltage noise.

As shown in refs. 253 and 254, the zero field-cooled state of YBCO superconducting thin films can be driven by an applied current to a lower potential equilibrium state at magnetic fields and temperatures far below the depinning transition. This new equilibrium state of the vortex lattice has a larger elastic coupling (pinning). Furthermore, the results obtained indicate that the virgin field-cooled state without the applied current is a metastable, more ordered state of the vortex lattice than the one attained by applying some driving current. The pinning of the virgin state can be enhanced by the current-driven creation of defects in the vortex lattice. This pinning enhancement introduces a memory effect: once the enhancement has occurred, the corresponding new vortex configuration is remembered in the film after the driving current is reduced.[253,254]

Van Otterlo *et al.*[247] found that the critical current exhibits a peak *both* across the Bragg glass to vortex glass transition *and* across the melting line. The peak is accompanied by a clear crossing of the *I–V* curves. At higher applied currents the disorder is averaged to reduced values, and in three dimensions the vortices reorder into a "moving solid."

Olson *et al.*[252] studied the dynamic phases of vortex matter in disordered highly anisotropic materials such as BSCCO. They observed a sharp 3D–2D transition from vortex lines to decoupled pancake vortices, as a function of the relative interlayer coupling strength. They found an abrupt large increase in the critical current as the 3D–2D line is crossed in a direction corresponding to increasing H, with decoupled pancakes being much more strongly pinned. As driving currents increase well above depinning, they found that the decoupled pancakes simultaneously recouple and reorder into a crystalline-like state.

Vortex melting. Vortex melting has long been the subject of intensive study (see, for example, Soibel *et al.*[255] and references therein). Recently, a very rare "inverse" melting process was reported.[256] This is a process in which a crystal reversibly transforms into a liquid or amorphous phase when its temperature is decreased. Search for this phase is usually hampered by the formation of non-equilibrium states or intermediate phases. However, by dithering vortices and thus equilibrating the vortex lattice, Avraham *et al.*[256] obtained direct thermodynamic evidence of inverse melting of the ordered lattice into a disordered vortex phase with decreasing temperatures. This work was done with the help of microscopic Hall sensors providing local magnetization measurements on high-quality BSCCO crystals. The mechanism of the first order phase transition changes gradually from thermally induced melting at high temperatures to a disorder-induced transition at low temperatures.

AC effects. Measurement of the ac response of superconductors immersed in an applied ac magnetic field has long been an important tool for studying flux dynamics and verifying flux pinning models. Recent developments in this area include the determination of the activation energy by ac susceptibility measurements,[257] studies on the plasticity and memory effects in the vortex system, also using ac susceptibility measurements,[258] the determination of the degree of order of the vortex solid under symmetric and asymmetric ac fields,[259] the thermal-to-quantum flux creep crossover in

different superconducting thin films,[260] studies of dynamic regimes in the ac response of YBCO with columnar defects,[261] dislocation-mediated creep of highly separated vortices,[262] higher harmonic ac susceptibility,[263] and the ac response of a finite thickness sample under a perpendicular magnetic field.[264]

Experiments described in ref. 265, where a small ac component was superimposed on a dc magnetic field, enabled an examination of the vortex–glass transition from a new point of view. In this work,[265] the vortex–glass transition temperature in YBCO films coincided with the temperature of the depinning transition. In the light of these experiments, an alternative explanation of the vortex–glass transition within the framework of percolative vortex motion[266–268] seems to be very attractive. However, more evidence is needed to completely settle the matter.

Superconductors of finite thickness in a perpendicular field. Magnetic measurements, such as magnetization hysteresis loops, magnetic relaxation and ac susceptibility have been widely used to study the flux dynamics of high temperature superconductors. As a result, critical current densities and activation energies, as well as the $U(J)$ relationship, have been determined experimentally by this contactless technique. Although magnetic measurements have the advantage of using contactless and non-destructive technology, experimentally, in order to get maximum signal, most magnetic data have been taken on thin films and single crystals, usually in the form of platelets, with the applied field perpendicular to the film plane. Unfortunately, the analysis of experimental data in this perpendicular field geometry is complicated by strong demagnetizing effects. Most of the models available are suitable only for infinite long samples in a parallel magnetic field.

Brandt[269–272] and other workers[264,273–276] have recently made detailed calculations of the response of superconductors of finite thickness in perpendicular magnetic fields. The Meissner–London currents of superconductor strips with a rectangular cross section in a perpendicular field,[273] the flux penetration, magnetization curves, linear and nonlinear ac susceptibility of disks and cylinders in an axial magnetic field,[269,270] geometric barrier effects, current string and irreversible magnetization of pin-free superconductors of finite thickness,[271,272] critical state in anisotropic superconductors of arbitrary shape with or without field-dependent or anisotropic pinning,[275,276] as well as the fundamental and harmonic ac susceptibility[274] have all been derived. The results demonstrate many interesting phenomena different from what was expected from the case of an infinite superconductor in a parallel magnetic field.

4.2 MgB_2 superconductors

The recent discovery of the superconductor MgB_2 with its transition temperature at 39 K has aroused considerable interest in the field of condensed matter physics, especially in the area of superconductivity. In the following, we present a brief review of the superconducting properties of this new material.

Magnetisation behaviour. *1 Upper critical field and coherence length.* A number of workers have found a definite anisotropy in the upper critical field (complete loss of superconductivity in the bulk) of MgB_2 in thin films,[277,278] single crystal,[12,13] aligned

crystallites,[279,280] and textured bulk[11] samples, with the ratio $\gamma = H_{c2}^{ab}(0)/ H_{c2}^{c}(0)$ (at 0 K) = $\xi ab/\xi c$ ranging from 1.7 up to approximately 2.6. $H_{c2}^{ab}(0)$ ranges from 11 T to 39 T (in a thin film sample),[278] and the coherence length ξ_{ab} ranges from 3.7 nm[277] to 7.0 nm.[279] γ values of approximately 8 with ξ_{ab} = 12.8 nm were obtained from conduction electron spin resonance measurements[281] on MgB_2. The upper critical field falls off in an approximately linear way with temperature, with the slope sample dependent. The graph is marked by a positive curvature near the critical temperature like some other boron intermetallics.[282–284]

Wang, Lim and Ong[285] were able to calculate upper critical fields in good agreement with experiment using a continuous Ginzburg–Landau model. They obtained a calculated order parameter, implying three-dimensional behaviour.

2 Lower critical field. Reported lower critical field values at or below 4 K range between 25 and 48 mT.[286,287] A value of 25 mT was found from microwave absorption.[288] $H_{c1}(T)$ is a linear function and has a finite slope down to 2 K, which is inconsistent with an isotopic *s*-wave superconductivity.[289]

3 Irreversibility line. Several groups have measured the irreversibility line for MgB_2 using magnetisation[282] and transport measurements.[290] $H_{irr}(T)$ is lower and more important for applications than $H_{c2}(T)$ because non-zero critical currents only occur below the irreversibility line. $H_{irr}(0)$ typically falls between 6 and 12 T for reports on bulk, films, tapes and powders. The irreversibility line is quite low in MgB_2 compared with high temperature superconductors. The activation energy for flux creep (the motion of vortices across pinning centers) decreases rapidly with increasing magnetic field compared to the copper oxide superconductors, implying generally weak flux pinning.[257] Flux creep near the irreversibility line was also investigated by Ghigo *et al.*,[291] with different conclusions reached on the activation energy.

4 Penetration depth. A study of the optical conductivity of MgB_2 by Pronin, Pimenov and Krasnovobodtsev[292] revealed qualitatively BCS-type behaviour including a peak in the temperature dependence of the real part of the conductivity above T_c. However the penetration depth $\lambda(T)$ showed a quadratic T dependence, indicating nodes or strong anisotropy in the superconducting gap. Panagopoulos *et al.*[293] also measured the magnetic penetration depth using muon spin rotation and low-field ac susceptibility. They found $\lambda(0)$ = 85 nm and also noted the quadratic temperature dependence.

5 Vortex dynamics. Bugoslavsky *et al.*[294] studied the vortex dynamics in MgB_2 using J_c and the vortex creep rate. They found that natural grain boundaries are highly transparent to supercurrent, unlike the copper oxide superconductors, but that currents fell off sharply with increasing magnetic field. Zhao *et al.*[295] measured the magnetisation relaxation of MgB_2 and found very weak flux creep and weak quantum tunneling, again unlike cuprate superconductors. These factors were suggestive of strong pinning. Kim *et al.*[296] note that the magnetisation curves of MgB_2 are well fit by the exponential critical state model, suggesting that the irreversible magnetisation is dominated by bulk pinning up to 0.9 T_c. The normalised magnetisation curves at different temperatures scaled, implying that the flux pinning mechanism does not change with temperature. Wen *et al.*[297] measured the magnetic relaxation of high quality films and found that the flux dynamics were effectively the same as in bulk samples, although the relaxation rate was higher.

Qin *et al.*[257] derived the vortex pinning potential of MgB_2 bulk samples using ac susceptibility measurements. They found that the activation potential declines steeply with the applied field as $U(B) \propto B^{-1.33}$, which accounts for the sharp drop in the critical current density with magnetic field in MgB_2 (see Fig. 7). This group also found[257] that pinning in MgB_2 is due to pinning centers arising from spatial fluctuations of the transition temperature (δT_c-pinning), while pinning due to mean free path fluctuations (δl-pinning) is not observed (see Fig. 8).

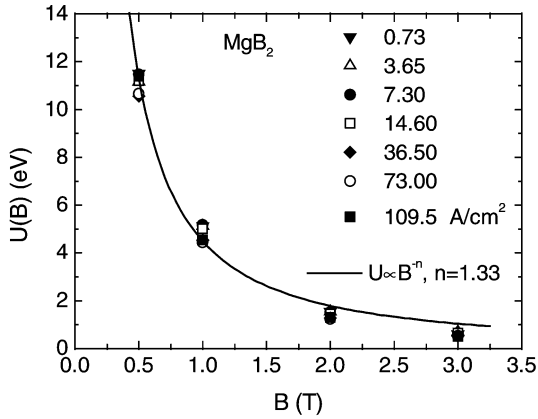

Fig. 7 Activation energy $U(B)$ as a function of the magnetic field for an MgB_2 bulk sample at various current densities. The solid line is the fitting curve $U(B) \propto B^{-1.33}$.

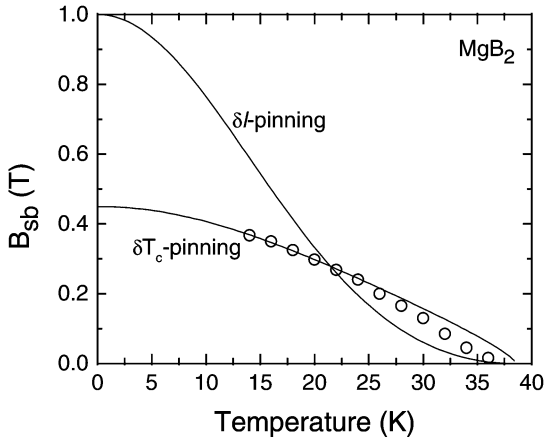

Fig. 8 Temperature dependence of the crossover field B_{sb} from single vortex pinning to small-bundle pinning. The δT_c –pinning line is in agreement with the experimental data, while the δl-pinning line is not.

Bugoslavsky *et al.*[294] blame the rapid decrease in J_c with magnetic field on an absence of natural defects. They report[298] a significant increase in pinning as a result of the atomic disorder produced by proton irradiation. Small enhancements in

pinning have also resulted[299,300] from thermal neutron irradiation (due to alpha particle emission by boron-10) and from heavy ion irradiation.[301] Kumakura *et al.*[7] found evidence that flux pinning occurs at grain boundaries, with small grain samples showing a higher irreversibility line.

Wen *et al.*[302,303] attribute the large separation between the irreversibility line and $H_{c2}(T)$ to the existence of a quantum vortex liquid state. Strong quantum fluctuations of vortices are responsible for the formation of the state and its later melting at higher temperatures. Bhide *et al.*[288] found evidence from absorbed microwave power of a transition from a strongly pinned flux lattice to a flux flow regime. Johansen *et al.*[304] were able to image flux penetration into a very good quality MgB_2 film using magneto-optical techniques. They found an abrupt invasion of dendritic flux structures at temperatures as low as 10 K, rather than a uniform and gradual flux penetration. Polyanskii *et al.*[305] also used magneto-optical imaging and found a uniform, Bean critical state magnetisation behaviour with almost no electromagnetic granularity.

6 Flux jumping. Flux jumping, first reported by Dou *et al.*,[306] is an instability seen in magnetisation hysteresis loops at low magnetic field and temperatures below 15 K. Flux jumping truncates the available magnetisation in these regions, and is related to penetration of the magnetic field at grain boundaries. It ends when the grains decouple with further increases in H and T.

Resistivity and conductance. Jung *et al.*[10] studied the temperature and magnetic field dependence of the resistivity of MgB_2. Like other workers[308] they found a quadratic temperature dependence in the normal state, but there was no dependence on magnetic field. The resistivity behaviour resembles that of a simple metal.[283] Kohen and Deutscher[309] measured the differential conductance versus voltage measurements of Au/MgB_2 point contacts. They found that the dominant component in the conductance was due to Andreev reflection.

Current flow. *1 Critical current.* The best critical current values reported[310,311] are in thin films and extend above 10^7 A cm^{-2} at 4.2 K, 0 T. These values are an order of magnitude better than in the best reported results for other forms of MgB_2 and for Nb_3Sn film. However, it should be noted[4] that J_c values fall off far more quickly with increasing magnetic field in MgB_2 than in Nb_3Sn, with the curves crossing at about 5 T.

2 Weak link behaviour. Larbalestier *et al.*[312] did a comprehensive study of supercurrent behaviour using magnetisation, magneto-optical and X-ray measurements. They found that supercurrents flow across the grain boundaries without being compromised by weak link problems. Other workers have made similar findings.[7,294,313–315]

5 Applications

5.1 Superconducting tapes and wires

Large-scale superconducting electric devices for the power industry depend critically on wires with high critical current densities (J_c) at temperatures where cryogenic losses are tolerable. This restricts choice to two HTS materials, $(Bi,Pb)_2Sr_2Ca_2Cu_3O_x$-(Bi:2223) and $YBa_2Cu_3O_x$(YBCO), and possibly to MgB_2. Crystal structure and

material anisotropy place fundamental restrictions on their properties, especially in polycrystalline form.[312] The feasibility of superconducting power cables, magnetic energy-storage devices, transformers, fault current limiters and motors, using Bi-2223, is proven. Widespread applications now depend significantly on cost-effective resolution of fundamental materials and fabrication issues, which control the production of low-cost, high performance conductors of these remarkable compounds.

High temperature superconducting tapes. The technical performance of Ag-clad $(Bi,Pb)_2Sr_2Ca_2Cu_3O_x$ (Bi:2223/Ag) and $Bi_2Sr_2Ca_1Cu_2O_x$ (Bi:2212/Ag) wires produced by numerous manufacturing companies have reached the levels required for the demonstration of some large-scale applications such as: AC power transmission cables, electric motors, generators, transformers, magnetic energy storage coils, and fault current limiters. Progress made in this area includes improvements in grain connectivity, texture, phase composition and flux pinning.[316]

The extremely high upper critical fields and high transition temperature make the HTS advantageous over conventional superconductors, in particular, for applications in the areas where high J_c in significant magnetic fields is essential. It is well accepted that J_c of HTS conductors is limited by multiple mechanisms operating simultaneously.[317] Because of this complexity, it is still not clear what the true limits to J_c in this system are. These multiple current limiting mechanisms can be classified into two relatively independent factors, the first factor being the grain connectivity and the second the flux pinning in the grain. The former determines the intergranular critical current and the latter is associated with intragranular critical currents. Furthermore, the conductor costs are still too high, partly because J_c is compromised by weak flux pinning in fields. Thus, it is vitally important to understand all the factors that influence J_c.

The Ag-sheathed Bi: HTS conductors referred to consist of multicore round wires and ribbons based on Bi-2212 and Bi-2223. Bi-2223/Ag multicore tapes are incorporated into all of the demonstration devices mentioned above. Several developments in Bi-2223/Ag powder-in-tube processing have been reported.[316,318] It was found that J_c is strongly dependent on core density and a number of techniques have shown to be effective[318] for increasing density as shown in Fig. 9. Further, the composition of phases formed during cooling have a significant effect on grain connectivity and flux pinning in the tapes.[319] The residual liquid phase and cracks are largely responsible for weak links, substantially reducing J_c. A two-stage annealing procedure in the final thermal cycle has been used to convert the liquid to Bi-2223. By incorporating hot-deformation in a two-step process, not only can the Bi-2201 phase be eliminated, but the texture and density are also improved, resulting in a high J_c, for example, 60 kA cm^{-2} at 77 K in multifilamentary tapes.

Another obstacle for HTS is that their J_c deteriorates rapidly with increasing temperature and magnetic field due to the thermally activated creep of magnetic flux. J_c vanishes at the irreversibility field, $H_{irr}(T)$, which is far below $H_{c2}(T)$ at 77 K. The most encouraging development is that both H_{irr} and J_c can be significantly improved, as demonstrated by the neutron irradiation of U-doped Bi:2223 tapes in which the fission tracks raise H_{irr} to over 1 T at 77 K, while reducing the anisotropy of J_c by two orders of magnitude in fields greater than 500 mT at 77 K.[320] Enhanced flux pinning has been introduced into some "uranium-doped" tapes by developing fission tracks in

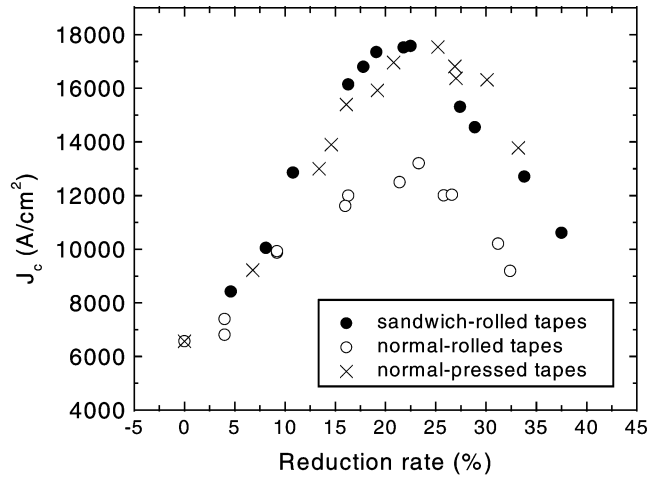

Fig. 9 J_c *versus* reduction rate for tapes processed using three intermediate methods: flat-rolling (FR), sandwich rolling (SR) and pressing (P).

them by thermal neutron activation — the "U/n" technique.[321] In a novel improvement upon earlier applications of the U/n method, the development of excess radioactivity has been substantially reduced through the use of $U(Sr_{1.5}Ca_{1.5})O_y$, a compatible compound with Bi-2223.[322,323] Columnar defects produced by heavy ion and proton irradiation are very efficient pinning sites, leading to vast improvements in J_c and shifts in the irreversibility line. However, heavy ion and proton beams are not readily available and are expensive to use. Much more promising is an irradiation technique first introduced by Weinstein *et al.*[321] In this approach, the extended defects (fission tracks) produced by the fission of neutron-irradiated U^{235} inclusions (briefly described as the "U/n process") in YBCO samples act as very effective pinning centres. Fission tracks induced *via* U/n processing into Bi-tapes resulted in[324,325] more than one order of magnitude enhancement of $J_c(H||ab)$ at 3 T and 250 times enhancement of $J_c(H||c)$ at 0.7 T. Furthermore, anisotropy was reduced by 23 times at 0.5 T (Fig. 10). An innovative improvement to the basic U/n approach was devised[322] by replacement of the usual $UO_{3.5}$ with dopants such as $UCa_{1.5}Sr_{1.5}O_6$ (Fig. 11). Neutron irradiation results in heavy overlapping of fission tracks around the large U particles, damaging the zero field J_c. In addition, the radioactivity of the irradiated silver sheath is still rather high for practical applications of this technique. There are two solutions to this difficulty. One is the very successful $UCa_{1.5}Sr_{1.5}O_6$ – based route indicated above that requires much lower neutron doses. If the U doping is performed through spray drying, the atomic level homogeneity of U will ensure highly uniform distribution of fission tracks after irradiation. The other would be the elimination of Ag entirely and its replacement by Ni which has a much lower thermal neutron cross section and isotopes that are either very stable or have very short half lives.

The long debated issue of J_c uniformity in Bi-2223 and Bi-2212 single filament tapes[326] has now found a continuation in even more sophisticated study of the *multifilament* tapes.[318,327–330] In the case of *single* filament tapes the experimental findings

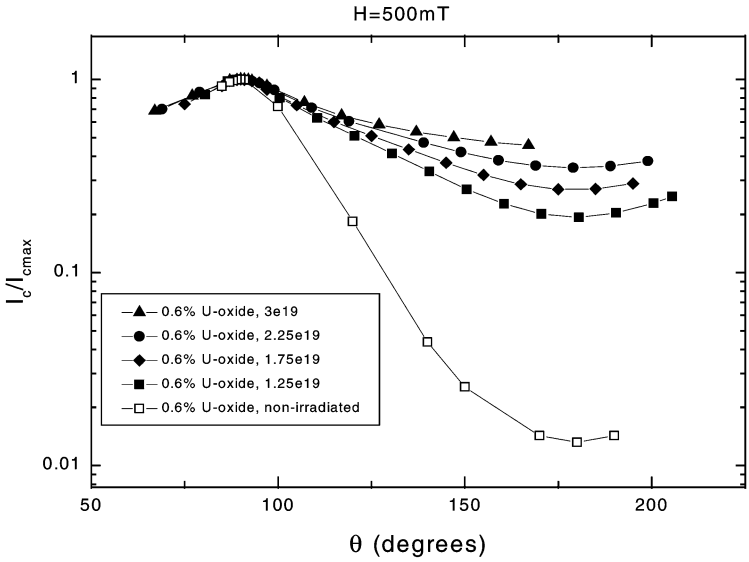

Fig. 10 Anisotropy of I_c and hence J_c before and after irradiation to various thermal neutron fluence for 0.6% U-doped Ag/Bi-2223 tape.

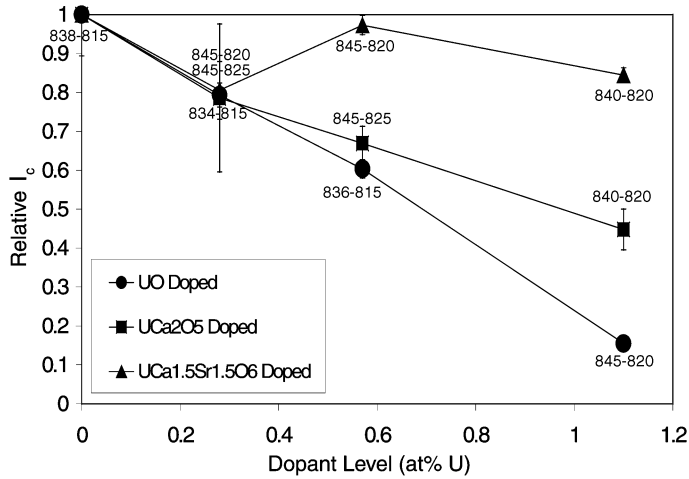

Fig. 11 Reduced I_c *vs*. uranium doping level for three uranium compound doping levels under optimised thermal processing conditions.

were quite diverse:[326] different regions of the superconducting core were found to carry a higher J_c than other core regions. This diversity has not yet found an unambiguous explanation. However, in the *multifilament* case, the majority of the experiments show that individual filaments situated centrally within the tapes have higher J_c values than the ones located on the periphery of the tapes.[318,327–330] Therefore,

by further tuning the manufacturing conditions a further overall J_c increase can be sought. Furthermore, the current distribution has been clearly shown to be influenced by intergrowth (the so-called bridging effect).[329–331] However, the influence of intergrowth on overall tape performance, including both current distribution and ac losses, has not been clearly identified yet.

Superconducting MgB_2 wires. Mechanical properties of MgB_2 material are similar to those of HTS cuprates: it is hard and brittle, not suitable for drawing into wires. Glowacki *et al.*[332] were the first to make highly dense wires and tapes by the powder-in-tube (PIT) technique using silver, copper, and bimetallic silver/stainless steel sheaths. In this technique powders are packed into tubes, which are then drawn and usually heat treated. Grasso *et al.*,[333] however, were able to produce J_c values as good as in bulk with dense, *unsintered* tapes sheathed in Ag, Cu and Ni. However, these results have not yetbeen reproduced by other groups. If heat treatment is used, Fe, Mo, Nb, V, Ta, Hf and W seem to be the most suitable for use with MgB_2 because other elements have problems with solubility and chemical reactions. Iron is likely to be the best prospect due to its ductility.[334] However, Cu-sheath was shown to exhibit some advantages over iron-sheath if a relatively higher mechanical deformation rate is applied,[335] which is encouraging for situations when non-magnetic sheath has to be used.

The production of iron tapes has been optimised by developing a reaction in-situ fast formation technique with mixed Mg and B powder-in-Fe tube.[336] In contrast to the common practice of long processing time, the results from this reaction *in situ* process show that there is no need for prolonged heat treatment in the fabrication of Fe-clad MgB_2 wires. A total time of several minutes at high temperatures is more than enough to form pure MgB_2 with high performance characteristics. A high magnetic J_c of 2×10^6 A cm^{-2} in zero field at 20 K and transport J_c of 50 000 A cm^{-2} at 1 T and 30 have been achieved (Fig. 12). As a result of such a short sint1ering period there is no need to use high purity argon protection, and it is possible to carry out the heat

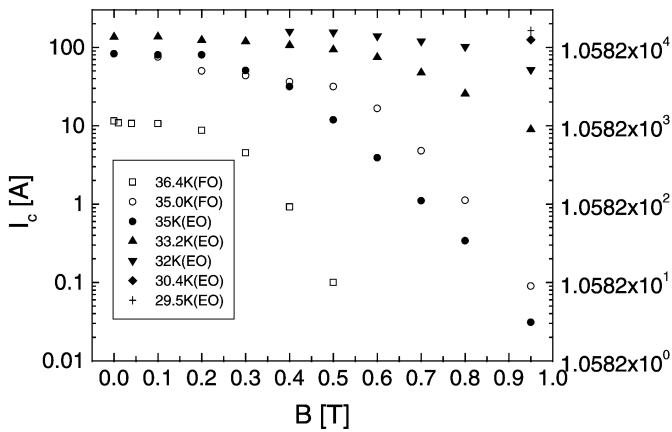

Fig. 12 Field dependence of I_c (left axis) and J_c (right axis) at different temperatures with field perpendicular (FO) and parallel (EO) to the tape plane.

treatment in a much less protective atmosphere. Because of such a short reaction time, not only are the crystals very small (several nanometres), but also the grain domains, which consist of clusters of crystals, are well below 100 nm. As reported in Wang *et al.*[337] large cluster domains formed during prolonged sintering decouple at high fields, resulting in a rapid drop in J_c. It has been shown[338] that both nanocrystalline and nanodomain boundaries are transparent to current, but that large domain boundaries create weak links (Fig. 13).

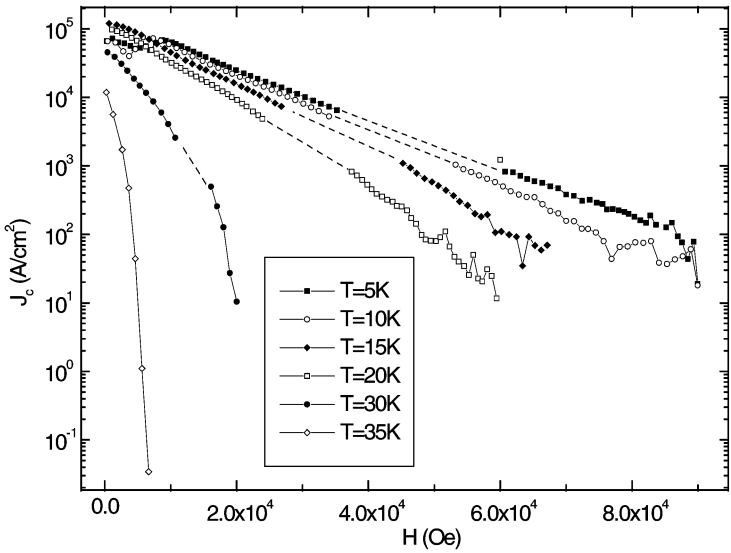

Fig. 13 Critical current density *vs*. field, with corrections for different screening lengths of the currents in small and high fields. In low fields J_c was calculated using the whole sample dimension, while the grain size was used in the high field region. The transient region in intermediate fields corresponds to the shape drop in the M–H loop due to the decoupling of the large grains.

Iron has been identified as not only compatible with MgB_2 but also an ideal magnetic screening material for reducing the effect of external fields and ac losses.[339] The screening can almost eliminate ac losses in fields up to 0.2 T. However, even beyond this field, there is a substantial reduction in ac losses,[340] currently by about a factor of 4. These results demonstrate clearly the great potential of the emergimg superconductor for various applications. However, the interaction between the magnetic sheath and the superconductor core remain unclear and should be explored. A better understanding of this may show new ways for lowering ac losses.

5.2 Fabrication of $YBa_2Cu_3O_{7-\delta}$ coated conductors

Coated conductors are a type of superconductor fabricated by epitaxial vapour deposition. A ribbon-like metallic substrate is used as support. The polycrystalline substrate could be non-textured, or could be cube-textured to decrease misorientation

of the polycrystalline film in the basal plane, and is approximately 0.1 mm thick. One or two buffer layers are often employed to prevent poisoning of the superconducting phase by the underlying substrate. The thickness of the buffer layers range from 50 nm to microns. Superconducting film approximately 400 nm thick is deposited on the top of the buffer layer/layers. Finally the superconducting film is covered with a protective metallic layer 1–5 μm thick. Manufacturing superconducting tapes by this method should allow long lengths to be fabricated for use in power applications such as motors, generators, transformers, magnets, power transmission and energy storage.

Much research has been focussed on producing long lengths of superconducting tape for power applications such as transmission lines, transformers, motors, generators, *etc*.[341–344] The brittle nature of superconducting oxide materials coupled with difficult processing techniques has proven a challenge to superconductor tape production.

The PIT technique was the first successful processing method for making long lengths of bismuth–strontium–calcium–copper oxide superconductors. This process has reached limits in terms of the maximum current density obtainable at a particular applied field for the length of wire that could be produced.[345]

The next advance in superconductor tape technology came with the development of Y-123 coated conductors. In order to minimize the decrease of current density caused by grain misorientation, there are two approaches: (1) the use of a randomly oriented substrate, onto which biaxially textured buffer and superconducting layers are grown; (2) the use of a cube-textured (also called biaxially textured) substrate onto which epitaxial buffer and superconducting layers are grown using vapour deposition. Under certain growth conditions, the resultant $YBa_2Cu_3O_{7-\delta}$ superconducting film does not suffer percolative current flow as in PIT processed superconductors. Also, the process can be scaled up to produce the long lengths of tape necessary in power applications.

Many substrate and buffer combinations have been developed. Silver and nickel are common substrate materials as a strong biaxial texture can be obtained by cold rolling to large reductions followed by annealing. Reactions between the substrate and superconducting film during processing require the use of buffer layers, which are metallic (silver, palladium, platinum) or ceramic materials (Y_2O_3-stabilised-ZrO_2, CeO_2, MgO, ZrO_2, $SmBa_2Cu_3O_{7-\delta}$, $La_{0.7}Sr_{0.3}MnO_3$).

A number of techniques are currently used for depositing the protective, buffer and superconducting layers: sputtering (rf, dc, magnetron),[346,347] pulsed laser deposition (PLD),[346–351] ion-beam-assisted-deposition (IBAD),[348,351,352] liquid-phase-epitaxy (LPE),[352,353] vapour-phase-solid (VPS) growth,[353] metal-organic-deposition (MOD),[352] electron beam evaporation,[351,354,355] inclined-substrate-deposition (ISD)[352] and ink-printed/floating zone heated method.[356]

Protective layer. A protective layer is often deposited last to protect the Y-123 layer. The main requirements for the protective layer are that it is chemically compatible with the superconducting film, is easily deposited and protects the surface from mechanical damage. The protective layer also allows the attachment of electrical contacts (necessary if ceramic buffer layers are used) and prevents moisture reacting with the superconducting film. A layer of silver or gold approximately 1–5 μm thick is typical.

The final tape is then annealed in flowing oxygen to lower the contact resistance between the protective layer and the Y-123 film and to obtain the orthorhombic (superconducting) phase and fully oxygenate the Y-123.[357]

Buffer layers. Buffer layers are required to prevent poisoning of the Y-123 superconducting layer by the underlying substrate material, and to provide the appropriate template for epitaxial growth of the Y-123 layer with an in-plane grain misorientation less than 8°.

Noble metals such as platinum, palladium or silver can be deposited onto the biaxially textured substrate at high rates, forming an epitaxial buffer layer.[358] The resulting noble metal film provides the required template for epitaxial growth of the oxide buffer layers or the superconductor directly.[345]

The good chemical compatibility of silver and Y-123 means that the superconducting layer can be deposited directly, without the need for complex buffer layers. Moreover, twinning could occur in the silver buffer layer, which would significantly degrade the superconducting properties.

For nickel substrates a combination of metal and ceramic buffer layers may be used. A multilayered film architecture is used, comprising Y_2O_3-stabilised-ZrO_2 (YSZ) and CeO_2 on the surface for improvement of the crystallinity of Y-123 and control of the chemical reaction between the metal substrate and the Y-123 film.[352] If exposed to an oxidising atmosphere, bare nickel tape will form a randomly oriented NiO layer. The CeO_2 layer is first deposited to suppress the formation of NiO. Surface smoothness of ZrO_2 buffer layers[359] and cracking in CeO_2 buffer layers have both been reported.[360] These cracks may be associated with the high deposition temperature of the CeO_2 layer in oxygen. Shi *et al.*[361] reported a considerable decrease in the temperature of epitaxial deposition of CeO_2 in $Ar+10\%H_2$, which should also be beneficial for a reduction in the grooving of the grain boundaries in Ni.

By controlling the oxidation temperature and oxidation atmosphere, Matsumoto[362] developed an epitaxial relationship between the underlying nickel substrate and the NiO. This technique is called surface-oxidation-epitaxy (SOE). Under certain growth conditions, the NiO layer can grow epitaxially on the textured Ni substrate, but the cracking of the oxide layer is apparently difficult to control.[363]

Substrate requirements. The main requirements for polycrystalline substrates refer to chemical stability under the deposition conditions, surface roughness and mechanical strength. These substrates are used in conjunction with buffer layers deposited in a biaxially textured form by pulsed laser deposition (PLD), with the required texture being formed by ion beam, in the so-called ion beam assisted deposition (IBAD).

Uniaxially aligned Y-123 films (*c*-axis $\perp$ substrates) are easily grown on polycrystalline substrates, but the superconducting properties are heavily degraded at grain boundaries. Weak coupling occurs due to grain misorientations.

If the angle θ defines the misorientation angle between adjacent grains in the basal plane, and the angle ϕ represents the misorientation angle between grains in the direction perpendicular to the basal plane, work by Dimos[364] showed that even if samples can be fabricated with almost perfect c-axis alignment (uniaxially aligned, $\phi \cong 0$), misorientations in the basal plane between adjacent grains will limit J_c.

By increasing the orientation both normal to and within the basal plane (biaxially aligned structure), an increase in current density can be obtained compared to uniaxially aligned substrates.[364]

Cube texture can be produced in many fcc metals and alloys of medium-high stacking-fault-energy (SFE) with excellent precision and sharpness. The cube texture can be found in copper, aluminium, silver, gold, nickel, iron–nickel (>30% nickel) alloys and iron–nickel–copper alloys. The cube texture in these materials is often so strong that it represents a single crystal, as the individual recrystallised grains are so closely oriented to the ideal orientation.[365] The number of conflicting experiments and different theories that exist on the formation of cube texture in fcc metals shows that the origin of cube texture in these metals is still a subject of controversy.[366] A detailed review of nucleation, recrystallisation and texture formation in polycrystals is given by Doherty.[367]

Although a highly oriented substrate is critical for coated conductor fabrication a number of other substrate requirements must be met.

1 Surface roughness. In order to successfully deposit the buffer and superconducting layers, the surface of the substrate must be smooth and flat. Any surface irregularities on the substrate will be duplicated in the buffer and superconducting layers if of sufficient size, resulting in degraded superconducting properties.

The principal factors affecting the surface quality of the substrate have been identified as rolling damage (function of roll roughness) and grain boundary grooving during annealing.[368]

The surface smoothness can be enhanced by mechanical and/or electrolytic polishing prior to deposition of the buffer and superconducting layers, although this may contaminate the surface and introduce strain into the grains.

Mechanical polishing alone can produce satisfactory surface smoothness. In the production of Inconel and Hastelloy substrates. Willis[357] obtained an average surface roughness of 100–300 nm at the conclusion of thermomechanical processing, which was reduced to 2–5 nm by mechanical polishing.

Mechanical polishing can cause contamination of the surface by means of polishing artifacts, and strain can be introduced into the grains due to plastic deformation of the abrading particles. The outermost layer of an abraded surface is equivalent to a material which has been severely cold rolled (99% reduction). This fragmented layer is composed of very fine sub-grains and contains a high density of defects.[369] The orientation of these subgrains is found to have characteristic textures.[370]

Electrolytic polishing can also be used to improve the surface smoothness. The surface to be electrolytically polished must be as flat as possible. This flatness requirement generally dictates that the sample must be subjected to some form of mechanical polishing prior to electrolytic polishing. The rate of material removal during electrolytic polishing is typically 1 μm min^{-1}, so long polishing times would be required to remove the damage introduced from the prior mechanical polishing step.[369] This means that electrolytic polishing itself does not ensure the production of an artifact free surface. Also, electrolytically polished surfaces will usually be contaminated by both the formation of a thin film due to the anodic surface as an essential part of the process and the possibility of absorption of complex ions either formed in the viscous layer during polishing or present in the polishing solution itself.[369]

It is anticipated that the surface roughness should not be greater than 1/10 of the buffer layer thickness (5–10 nm).

2 Mechanical properties. The comparatively strong, ductile metal substrate must support the more brittle oxide superconductor.[360] The coated conductor must have sufficient mechanical strength to allow fabrication into superconducting devices. Much of this mechanical strength is imparted by the substrate. Many applications do create significant mechanical stress on the coated conductor as it forms an integral part of the design, incorporating cooling and other structural elements.

In a study of Inconel/YSZ/Y-123 superconductors performed by Thieme *et al.*[371] it was shown that at 77 K up to 0.5% strain does not change J_c by more than 3%. This strain dependence is better than the tensile stress dependence of J_c when the samples are bent at room temperature.[371]

3 Grain size. It is desirable to have as large a grain size as possible, as grain boundaries degrade superconducting properties. It is also desirable for the grain size formed during cold rolling and annealing to remain stable during further processing. There are many possible substrate materials including silver, nickel, copper and alloys of these materials. Whilst all of these metals develop cube texture from thermo-mechanical processing, they all offer different mechanical, physical and chemical properties.

Textured Ag. The early work involving the epitaxy of Y-123 films vapour deposited onto bulk single crystals of silver is covered in the work of Budai *et al.*[372] Hence efforts were directed towards producing a substrate material with a sharp biaxial texture using rolled silver, since silver is one of the few metals with benign interactions with high temperature superconductors.[345] Some success has been achieved using cold rolling and recrystallisation[373] and hot rolling and recrystallisation.[368,373]

It has been found that Y-123 grows with a single orientation on the (110) plane of silver, so that the ideal recrystallisation texture would be one which orients this plane parallel to the surface of the tape.[368,372,373] Typical rolling textures in silver correspond to the brass texture having orientations of {110}<112> and {236}<385>.[345] Under controlled deformation rates, annealing conditions and initial billet oxygen contents, several researchers have obtained the {110}<110> texture in silver[368,373] and silver alloys.[373] However, there is some twinning present, which decreases J_c. Since the twins most likely nucleate and recrystallise from stacking faults in the as rolled silver, improved texture should be possible by increasing the stacking fault energy of the silver through doping additions and oxygen control.[373] Alloying is also necessary to increase the mechanical strength of the tape.[352,368]

The cube texture {001}<100> has been obtained in silver by Doi *et al.*[374] by warm rolling and subsequent annealing at 700–850 °C. These tapes have been referred to as cube-textured silver tape (CUTE tapes) and have been manufactured in 80 m lengths with grain boundary misorientation angles of only a few degrees.

Further work is still required with silver substrates to sharpen the texture, reduce twin component and increase mechanical properties.[352,368,373]

Textured nickel substrates. In order to avoid the problems associated with texturing silver directly many researchers have performed thermomechanical processing of fcc base metals such as nickel.[345,349,352,375–379]

A biaxially textured buffer layer can be easily grown on surface of nickel or nickel alloy tapes with {001}<100> orientation. The development of nickel substrates was rapidly advanced by Goyal *et al.*[380] who fabricated long lengths of superconducting tape, referred to as rolling-assisted-biaxially-textured-substrates (RABiTS™). Work by Truchan *et al.*[377] showed that nickel sheets uniformly rolled to >95% reduction developed a sharp cube texture for all heat treatments between 400 and 1000 °C, showing slight improvement with longer annealing times. Recrystallisation studies in cold rolled pure nickel performed by Makita *et al.*[378] showed that the primary recrystallisation texture produced during high temperature annealing of heavily cold rolled nickel sheets was an extremely sharp cube texture, independent of initial grain size and depth from the sheet surface. The sharpness of the cube texture is found to increase with higher percentage rolling reductions.[376]

Texture studies performed by Petrisor *et al.*[376] revealed that the {001}<100> cube texture can be easily developed in Ni–V alloys (up to 11 at.% vanadium) by a cold rolling process followed by a thermal recrystallisation treatment.

The technological issues concerning nickel substrates are related to the mechanical strength and magnetism of nickel. Various approaches to the fabrication of stronger substrates with reduced magnetism have been suggested, including composite structures and alloys.[352]

Textured copper substrates. After heavy deformation of copper the primary texture is {112}<111> with small traces of {001}<100>. On annealing it is the {112}<111> texture which is the host for the cube texture, which is nucleated by the traces of cube texture in the as-deformed material. The first requirement for a strong annealing texture is thus a minor texture component accompanying the major deformation texture.[380]

Little work to date has focused on developing coated conductors using cube textured copper substrates. However, researchers have highlighted the possibility.[343]

For biaxially textured substrates, the following specifications can be used as a guideline:[358]

{001}<100> cube texture fraction, as determined from normalized X-ray pole figure, >97%.

{001}<100> cube texture fraction variation along the lengths, as determined from normalized X-ray pole figure, <2%.

{122}<212> twin-of-cube texture fraction, as determined from normalized X-ray pole figure, <2%.

Out-of-plane texture variation, as determined by X-ray θ–2θ, (111)/(200)<1%.

Out-of-plane texture variation, as determined by X-ray φ scan, FWHM<8°.

In-plane texture variation, as determined by X-ray φ scan, FWHM<10°.

Average roughness, as determined by AFM, R_a<25 nm.

Results on biaxially textured polycrystalline substrates. Substrates with biaxially textured, chemically compatible surfaces for epitaxial growth of superconducting materials were pioneered by Goyal[380] and are referred to as rolling-assisted-biaxially-textured-substrates (RABiTS). By using a biaxially textured substrate the speed of formation of biaxially textured buffer and superconducting layers is greatly

enhanced.[352] Long lengths of biaxially textured substrate can be produced by thermomechanical processing.

Thermomechanical processing of fcc metals such as silver, nickel and copper result in biaxially textured substrates for Y-123 coated conductors as their lattice parameters are close to the *a* and *b*-axis length of the Y-123 crystal.[352] Y-123 has lattice parameters: $a = 3.82$ Å, $b = 3.89$ Å and $c = 11.69$ Å. The *a*-axis length of silver, copper and nickel are 4.09 Å, 3.62 Å and 3.52 Å respectively.

Park *et al.*[381] deposited a single 250 nm YSZ buffer layer directly onto short, 50 μm thick, biaxially-textured Ni substrate by PLD, followed by the deposition of a Y-123 layer, also by PLD. They achieved a satisfactory in-plane and out of plane texture, yielding a J_c of 1 MA cm^{-2} at 77 K in 0 T.

Recently it was shown[382] that the metal organic deposition (MOD) process can be employed to grow buffer layers of $SrTiO_3$ onto biaxially-textured Ni substrate. However, the grown layer has a mixed texture, with a strong cube component as well as a random component, which clearly indicates the necessity of further investigations.

Fabbri *et al.*[383] studied the epitaxial growth of Y_2O_3 and CeO_2 by electron beam evaporation (EBE) and PLD onto short lengths of biaxially-textured, non-magnetic Ni–V alloy. The orientation of the buffer layers yielded similar results for the two deposition methods, with an ω-scan FWHM of 7.5°.

In order to circumvent the problem of deteriorating microstructure in the Y-123 layer above approximately 1–1.5 μm, Foltyn *et al.*[384] introduced a corrective layer of $SmBa_2Cu_3O_{7-\delta}$ after each 1 μm of Y-123 layer. Using this approach, an I_c in excess of 400 A per cm width of the tape was obtained for a multilayer Y-123 architecture (Y–Sm–Y–Sm–Y) with a total thickness of 3.7 μm, and a J_c of 1.1 MA cm^{-2}.

The use of conductive buffer layers also has the advantage of stabilizing the conductor against thermal runaway. Aytug *et al.*[385] used a single conductive buffer layer of $La_{0.7}Sr_{0.3}MnO_3$ deposited by magnetron sputtering onto a short, biaxially textured Ni substrate. Measured by φ-scan, the FWHM of the buffer layer was 9.7°. A superconducting Y-123 layer was deposited by PLD, and yielded a J_c of 0.5 MA cm^{-2} at 77 K and 0 T.

On short samples of biaxially textured Ni and NiCr substrates, Li *et al.*[386] used EBE for a CeO_2 or YSZ buffer layer, and MOD for a 0.4 μm thick Y-123 layer. The J_c obtained for this sample was 2.1 MA cm^{-2} at 77 K and 0 T.

Results on non-textured polycrystalline substrates. A major step in the development of strongly linked superconductors with high critical currents was made by Iijima *et al.*[387,388] and Reade *et al.*[389] with the oxide superconductor $YBa_2Cu_3O_{7-\delta}$ (Y-123). Using IBAD they deposited biaxially textured ceramic buffer layers on polycrystalline, randomly oriented, Hastelloy tapes. Epitaxial deposition of Y-123 onto the biaxially textured buffer layer resulted in films with primarily small angle grain boundaries and a value of J_c in excess of 10^5 A cm^{-2} (77 K, 0 T). Work performed by Wu *et al.*[390] improved the in-plane alignment of the IBAD layer and hence the Y-123 film, with a resultant increase in J_c to values exceeding 10^6A cm^{-2}.

Work by Nakamura *et al.*[391] showed that liquid phase epitaxy (LPE) could be a viable method for fast growth of the Y-123 layer, in conjunction with a MgO buffer layer obtained by PLD-IBAD or inclined substrate deposition (ISD) on non-textured

Hastelloy C. In order to prevent the dissolution of MgO into the Y-123 layer, an intermediary layer was also grown by LPE, composed of MgO-rich Y-123.

Using a scaled-up process, Iijima *et al.*[392] successfully deposited a biaxial YSZ buffer layer onto a 3 m long Hastelloy ribbon by IBAD at a speed of 0.25 cm h^{-1}, achieving an in-plane mosaic spread of 17°–19° along the entire length. Y-123 was deposited onto this template by PLD at a speed of 4 m h^{-1}, achieving a J_c of 2.4×10^5 A cm^{-2} at 77 K and 0 T, even with such a relatively large in-plane misorientation.

Willis *et al.*[357] produced biaxial YSZ on 1 m long Inconel and Hastelloy by IBAD. The surface roughness of the metallic substrate was R_a<6 nm obtained by mechanical polishing. A PLD process was used to deposit 1 μm thick Y-123 film at a speed of 0.25 m h^{-1}, achieving a J_c of 1 MA cm^{-2} at 77 K and 0 T, with critical current I_c of 122A. Using MgO as an IBAD template, the deposition time was reduced by one order of magnitude for the entire length. This was based on previous work, which showed that the biaxial texturing mechanism of MgO takes place at the nucleation stages of the film,[393] as opposed to the biaxial texture of the YSZ, which improves gradually, as the thickness of the film is increased. For this reason, only approximately 10 nm of MgO buffer layer is required, rather than 500 nm or more of YSZ.

A high coating rate of Hastelloy by MgO was achieved with electron beam evaporation (EBE) using the inclined substrate deposition (ISD) technique.[394] The reel-to-reel MgO coating rate was as high as 0.6 μm min^{-1}, yielding a thickness of 1 μm in a single pass. In-plane orientation of the MgO layer determined from a φ-scan, showed a reasonable FWHM of 10°–12°.

A most encouraging result comes from Sumitomo Electric, which produced a 3 m long Y-123 tape on YSZ template, deposited by ISD onto Hastelloy,[395] with a reported J_c higher than 10^4 A cm^{-2} at 77 K and 0 T.

Metallic buffer layers as well as Ag substrates are very promising. On short lengths of 1 cm polycrystalline Ag, a 0.14 μm thick film of Y-123 was directly deposited by ISD, yielding a J_c of 2.7×10^5 A cm^{-2}.[396]

Foltyn *et al.*[397] used IBAD to grow biaxially textured YSZ onto non-textured Inconel substrate 1m long. Further, another buffer layer, Y_2O_3 or CeO_2 was deposited by PLD, as well as a 1.4 μm thick Y-123 film. This conductor had a critical current I_c of 122 A at 77 K, with a variation of ±20%.

Ignatiev *et al.*[398] made a comparative study of different substrates: $LaAlO_3$, non-textured Ni with IBAD processed YSZ and biaxially textured Ni, onto which buffer CeO_2 or YZS layers, as well as Y-123 film were grown by photo-assisted MOCVD, at a growth rate of 0.5 μm min^{-1}. On $LaAlO_3$, the typical ω-scan FWHM for both CeO_2 and YZS is approximately 1°. On biaxially-textured and non-textured Ni, the in-plane orientation of the buffer layers was less sharp than on the single crystal substrate, but the actual value was not indicated.

Usoskin *et al.*[399] reported a 2 m long and 9.2 mm wide Y-123 tape deposited by PLD on coated stainless steel, with an I_c of 142 A, corresponding to a J_c of 1.23 MA cm^{-2}.

Yamada *et al.*[400] used PLD-IBAD to deposit YSZ and CeO_2 buffer layers on short, non-textured Hastelloy substrates, and a solution approach, MOD, for the Y-123 layer. The J_c result for this sample was 1.7 MA cm^{-2}. The refined MOD technique used in this study achieved an impressive 7 MA cm^{-2} at 77 K and 0 T for Y-123 deposited on $LaAlO_3$ single crystal substrate.

The latest results for ISD come from Ma *et al.*,[401] who achieved a very high degree of in-plane alignment for a 2 μm thick MgO layer grown on short Hastelloy substrates, with a φ-scan FWHM of 12°, and a ω-scan FWHM of 6.3°. The J_c of this sample was 2×10^5 A cm^{-2} at 77 K and 0 T.

5.3 Devices using high temperature superconductors

Existing applications in the high temperature range all relate to copper oxide superconductors, although high quality tapes and wires have been made from MgB_2, so there is a strong possibility that this material will also find its way into applications in the future. Low temperature (LTS) superconductors found their way into serious use in electromagnets and other applications in the 1960s. There were thus very high hopes for the high temperature (HTS) copper oxide superconductors from the time they were discovered in 1986 by Bednorz and Müller.[150] This was because of the very much lower costs of refrigeration at liquid nitrogen temperature and because the mechanisms for this new type of superconductivity were not well understood, leading to hopes that it might be possible to find a room temperature superconductor. In reality, formidable materials science problems had to be solved, largely due to the ceramic, granular, anisotropic nature of the HTS materials. They are all very brittle and difficult to shape, and need to be formed at high temperatures in the presence of oxygen. Significant supercurrents can only flow along the CuO_2 planes, and it is difficult to ensure that all the grains in a finished device are correctly oriented. Impurities collecting at the grain boundaries cause weak link problems, resulting in reduced inter-grain currents. The grain boundaries also enable fast flux creep or vortex penetration into the materials. Flux pinning is difficult because of the unusually small coherence length, compared to the LTS materials.

Small-scale applications of HTS superconductors. Until very recently, the greatest success was achieved with small-scale electronic applications, and these are still commercially important. These devices mostly rely on the special properties of superconductors, especially Josephson quantum tunnelling effects. They are based on patterned thin films grown on a substrate. YBCO ($YBa_2Cu_3O_{7-x}$) is the most commonly used superconductor for this purpose because it has a high critical temperature (~92 K) and can carry high current densities. TBCCO ($Tl_2Ba_2CaCu_2O_y$) ($T_c \geq 100$ K) is also used, particularly in microwave communications applications, although TBCCO films are difficult to pattern due to the toxicity of thallium.[402,403] The materials for these films have largely been perfected, although it is still difficult to incorporate HTS superconductors into integrated circuits, due to grain boundary effects and problems with degradation of the underlying layers when attempts are made to grow multi-layer circuits. That is why niobium LTS superconductors are used for devices incorporating RSFQ (rapid single flux quantum) logic. For devices that do not require multi-layer circuits, the remaining engineering challenges relate to the vacuum packaging and the cryocoolers that are used to refrigerate the devices and keep them superconducting.[404] LTS materials are also used for similar small-scale devices, but the HTS devices have the advantage of smaller size, less complex refrigeration and smaller power consumption.

The main small-scale HTS electronic devices can be divided into (a) SQUID (superconducting quantum interference device) magnetometers (and instruments built from them) and (b) microwave filters and resonators for wireless telecommunications. Other applications include low noise sensing coils in NMR spectrometers, consisting of spirals patterned on YBCO film[405] and radiation detectors.[406] SQUID devices contain a ring of superconductor material with one or more Josephson junctions. When a current exceeding the critical current of the Josephson junction is introduced into a SQUID, a voltage appears that is proportional to the magnetic flux through the ring. SQUIDs can also detect any other physical quantities that can be converted to a magnetic flux. Superconducting magnetometers are orders of magnitude more sensitive than conventional devices and can detect magnetic fields 100 billion times smaller than that of the Earth. SQUID magnetometer devices have gone through considerable refinement in design but still work on the same principles.[407] SQUIDs are used in biomagnetic applications, such as magnetoencephalography (MEG) and magnetocardiography (MCG), geomagnetic measurements, and the magnetic and physical properties measurement systems used in materials science. Other applications include non-destructive testing applications, such as scanning SQUID microscopes used in testing chip packages in the semiconductor industry.[404]

Other small-scale devices include HTS passive RF and microwave filters used in telecommunications, particularly cellular networks. These devices are largely based on conventional microstrip and cavity designs, with the superconductor forming the microstrip or lining the metal cavity. The HTS filters have the advantages of very low noise and much higher selectivity and efficiency than conventional filters. There is now a large German research program aimed at using these filters in satellite communications because they minimise mass and volume compared to the bulky waveguides currently in use. They also minimise losses and noise figures, giving reduced power consumption and improved transmission capacity, and optimise spectral efficiency.[408]

Large-scale applications. Large-scale applications of HTS superconductors present an even greater materials science challenge than the small-scale applications. Devices have to be much bigger and must carry far larger currents, with current densities well above 10^4 A cm^{-2} for most applications, as well as working in far greater magnetic fields. These would range from about 0.2 T for a transmission cable to 4 T or above for a generator. Bulk materials are used for some applications, such as current leads to superconducting magnets,[409] but for most applications, the brittle ceramic superconducting materials must somehow be formed into long, flexible wires and tapes, which will stay superconducting throughout their length. A great deal of this challenge has been met by optimising the PIT method as discussed in Vase *et al.*[410] Larbalestier *et al.*[411] have written an extensive review on the feasibility of HTS superconductors for electric power applications, while the devices are reviewed in Hassenzahl.[412] For further information and references, see the section on tapes and wires and the section on coated conductors in this review.

Until very recently, YBCO was not considered suitable for large-scale applications because it is difficult to grow in bulk, but melt textured bulk YBCO is now being used to make quasi-permanent magnet prototypes that are of considerable current interest for Maglev trains, flywheels and motors.[413,414] The materials most commonly used in large-scale applications are the two main BSCCO superconductors, Bi-2212

($Bi_2Sr_2Ca_1Cu_2O_{8+x}$, $T_c \sim 85$ K) and, more importantly, Bi-2223 ($Bi_2Sr_2Ca_2Cu_3O_{10+x}$, $T_c \sim 110$ K), usually with some Pb doped into the Bi sites to stabilise the formation.

The main potential large-scale applications involve magnets for various purposes, power transmission lines, fault current limiters, generators and transformers for electrical utilities, large motors and flywheels. Some of these applications are already in use in demonstration projects while others have been developed to the prototype stage. The main remaining barriers are cost and concerns about performance in high magnetic fields at 65–80 K.[411] Most large-scale applications, apart from fault current limiters, simply involve the replacement of conventional copper conductors by superconductors. Fault current limiters[415,416] depend on the fact that superconductivity is lost and resistance reappears above a critical current. Under ordinary conditions a fault current limiter stays superconducting and passes current with no impedance. During a power surge the large fault current exceeds the critical current, forcing the superconductor to go normal, thus causing enough resistance to reappear to limit the fault current.

Magnet applications. Apart from the bulk YBCO magnets just mentioned, most superconducting magnets are basically electromagnets, with the copper coil replaced by a coil of superconducting wire or tape. Their main advantages are the elimination of energy losses due to resistance, higher magnetic fields than are attainable with conventional electromagnets,[417] and the fact that a magnetised superconducting magnet can be converted to a permanent magnet by disconnecting it from its current source and short circuiting the winding. The main disadvantage is cost, but where resistance losses are very significant, as in magnetic separators, where power consumption can be reduced by a factor of 20, superconducting magnets have already supplanted their conventional rivals.[418] Because of their greater efficiency, superconducting windings are almost invariably used in magnetic resonance (MRI) magnets in medicine where fields are above 0.3 T.[419] They are also commonly used in magnetic energy storage systems. In all these applications, however, the superconducting magnets in commercial use are LTS magnets. HTS magnets have the potential[420] to cut the power used for refrigeration by a factor of 100 and to be smaller, less complex, and easier to maintain and operate, but the superconducting windings are far more expensive. Although HTS prototype magnetic separators have been designed,[421,422] so far none are in commercial use. Prototypes are also under development for various magnetic levitation applications, such as flywheel bearings[423] and Maglev trains, as discussed above.

Generators, transformers, motors. Prototype generators,[424] including a novel high voltage generator,[425] transformers[426,427] and large motors[428,429] using HTS windings and bulk HTS materials are currently being designed and tested. As in the magnet applications, energy losses in the windings and armature bars are eliminated, giving massive gains in efficiency, and allowing the size and weight of the finished device to be reduced to a third that of its conventional equivalent. An HTS transformer would have the added advantage of being more environmentally friendly, as it would be oil free.

Power transmission. Power transmission cables made of superconducting Ag-sheathed Bi-2223 tape[430] are already in production. They are currently being used in

demonstration programs in Copenhagen (NKT Cables and Copenhagen Energy) and Detroit (American Superconductor and Pirelli) in utility substations. The cables are cooled to superconducting temperature by passing liquid nitrogen through their cores, and the BSCCO in them transmits as much current as 72 times their weight in copper. The extra cost of the HTS cable is likely to be justified in crowded cities where the alternative is digging up and replacing the existing conduits to upgrade capacity.

BSCCO current leads are also very close to viability.[431,432] Usually made of Ag alloy sheathed Bi-2223 tape or bulk BSCCO material, the current leads are designed to work as part of large LTS magnet systems, such as for magnetic energy storage. Their current carrying capacity is vastly greater than that of copper so that their cross-section can be much smaller. This means that they not only eliminate energy losses due to resistance, but energy losses due to heat transport into the 4 K environment of the LTS magnet.

Acknowledgements

The authors would like to thank Mr B. Winton for his contribution to the preparation of some figures in this report and to the Australian Research Council for financial support.

References

1 J. M. Schön, C. Kloc and B. Batlogg, *Nature*, 2000, **408**, 549.
2 R. J. Cava, *Nature*, 2000, **408**, 23.
3 J. Nagamatsu, N. Nakagawa, T. Muramaka, Y. Zenitani and J. Akimitsu, *Nature*, 2001, **410**, 63.
4 C. Buzea and T. Yamashita, *Supercond. Sci. Technol.*, 2001, **14**, 115.
5 S. C. Li, J. L. Zhu, R. C. Yu, F. Y. Li, Z. X. Liu and C. Q. Jin, *Chin. Phys.*, 2001, **10**, 338.
6 Z. A. Ren, G. C. Che, Z. X. Zhao, H. Chen, C. Dong, Y. M. Ni, S. L. Jia and H. H. Wen, *Chin. Phys. Lett.*, 2001, **18**, 589.
7 H. Kumakura, Y. Takano, H. Fujii, K. Togano, H. Kito and H. Ihara, *Physica C*, 2001, **363**, 179.
8 N. N. Kolesnikov and M. P. Kulakov, *Physica C*, 2001, **363**, 166.
9 C. U. Jung, M. S. Park, W. N. Kang, K. H. P. Kim, S. Y Lee and S. I. Lee, *Appl. Phys. Lett.*, 2001, **78**, 4157.
10 C. U. Jung, M. S. Park, W. N. Kang, K. H. P. Kim, S. Y. Lee and S. I. Lee, *Physica C*, 2001, **353**, 162.
11 A. Handstein, D. Hinz, G. Fuchs, K. H. Muller, K. Nenkov, O. Gutfleisch, V. N. Narozhnyi and L. Schultz, *J. Alloys Compounds*, 2001, **329**, 285.
12 M. Xu, H. Kitazawa, Y. Takano, J. Ye, K. Nishida, H. Abe, A. Matsushita, N. Tsujii and G. Kido, *Appl. Phys. Lett.*, 2001, **79**, 2779.
13 S. Lee, H. Mori, T. Masui, Y. Eltsev, A. Yamamoto and S. Tajima, *J. Phys. Soc. Jpn.*, 2001, **70**, 2255.
14 K. H. P. Kim, J. H. Choi, C. W. Jung, P. Chowdhury, H. S. Lee, M. S. Park, H. J. Kim, J. Y. Kim, D. Zhonglian, E. M. Choi, M. S. Kim, W. N. Kang, S. I. Lee, G. Y. Sung and J. Y. Lee, *Phys. Rev. B*, 2002, **65**, 100510.
15 H. J. Kim, W. N. Kang, E. M. Choi, M. S. Kim, K. H. P. Kim and S. Lee, *Phys. Rev. Lett.*, 2001, **8708**, 7002.
16 D. K. Aswal, K. P. Muthe, A. Singh, S. Sen, K. Shah, L. C. Gupta, S. K. Gupta and V. C. Sahni, *Physica C*, 2001, **363**, 208.
17 H. Y. Zhai, H. M. Christen, L. Zhang, M. Paranthaman, P. H. Fleming and D. H. Lowndes, *Supercond. Sci. Technol.*, 2001, **14**, 425.
18 Z. K. Fan, D. G. Hinks, D. G. Newman and J. M. Rowell, *Appl. Phys. Lett.*, 2001, **79**, 87.
19 L. H. He, G. Q. Hu, P. L. Zhang and Q. W. Yan, *Chin. Phys.*, 2001, **10**, 343.
20 G. Y. Sung, S. H. Kim, J. Kim, D. C. Yoo, J. W. Lee, J. Y. Lee, C. U. Jung, M. S. Park, W. N. Kang, Z. L. Du and S. I. Lee, *Supercond. Sci. Technol.*, 2001, **14**, 880.
21 S. Margadonna, T. Muranaka, K. Prassides, I. Maurin, K. Brigatti, R. M. Ibberson, M. Arai, M. Takata and J. Akimitsu, *J. Phys.: Condens. Matter*, 2001, **13**, 795.
22 R. C. Yu, S. C. Li, Y. Q. Yang, X. Kong, J. L. Zhu, F. Y. Li, Z. X. Liu, X. F. Duan, Z. Zhang and C. Q. Jin, *Physica C*, 2001, **363**, 184.
23 J. Q. Li, L. Li, Y. Q. Zhou, Z. A. Ren, G. C. Che and Z. X. Zhao, *Chin. Phys. Lett.*, 2001, **18**, 680.

24 R. F. Klie, J. C. Idrobo, N. D. Browning, K. A. Regan, N. S. Rogado and R. J. Cava, *Appl. Phys. Lett.*, 2001, **79**, 1837.
25 Y. Zhu, L. Wu. V. Volkov, G. Gu, A. R. Moodenbaugh, M. Malac, M. Suenaga and J. Tranquada, *Physica C*, 2001, **356**, 239.
26 F. Cordero, R. Cantelli, G. Giunchi and S. Ceresara, *Phys. Rev. B*, 2001, **6413**, 2503.
27 V. Milman and M. C. Warren, *J. Phys.: Condens. Matter*, 2001, **13**, 5585.
28 A. K. M. A. Islam and F. N. Islam, *Physica C*, 2001, **363**, 189.
29 M. Monteverde, M. Nunez-Regueiro, N. Rogado, K. A. Regan, M. A. Hayward, T. He, S. M. Loureiro and R. J. Cava, *Science*, 2001, **292**, 75.
30 J. Tang, L. C. Qin, A. Matsushita, Y. Takano, K. Togano, H. Kito and H. Ihara, *Phys. Rev. B*, 2001, **6413**, 2509.
31 B. Lorenz, R. L. Meng and C. W. Chu, *Phys. Rev. B*, 2001, **6401**, 2507.
32 I. Loa and K. Syassen, *Solid State Commun.*, 2001, **118**, 279.
33 E. Saito, T. Takenobu, T. Ito, Y. Iwasa, K. Prassides and T. Arima, *J. Phys.: Condens. Matter*, 2001, **13**, 267.
34 T. Tomita, J. J. Hamlin, J. S. Schilling, D. G. Hinks and J. D. Jorgensen, *Phys. Rev. B*, 2001, **6409**, 2505.
35 S. Deemyad, J. S. Schilling, J. D. Jorgensen and D. G. Hinks, *Physica C*, 2001, **361**, 227.
36 V. G. Tissen, M. V. Nefedova, N. N. Kolesnikov and M. P. Kulakov, *Physica C*, 2001, **363**, 194.
37 K. Prassides, Y. Iwasa, T. Ito, D. H. Chi, K. Uehara, E. Nishibori, M. Takata, M. Sakata, Y. Ohishi, O. Shimomura, T. Muranaka and J. Akimitsu, *Phys. Rev. B*, 2001, **6401**, 2509.
38 A. F. Goncharov, V. V. Struzhkin, E. Gregoryanz, J. Z. Hu, R. J. Hemley, H. K. Mao, G. Lapertot, S. L. Bud'ko and P. C. Canfield, *Phys. Rev. B*, 2001, **6410**, 509.
39 (*a*) J. D. Jorgensen, D. G. Hinks and S. Short, *Phys. Rev. B*, 2001, **6322**, 4522; (*b*) T. Vogt, G. Schneider, J. A. Hriljac, G. Yang and J. S. Abell, *Phys. Rev. B*, 2001, **6322**, 505.
40 A. K. M. Z. Islam, F. N. Islam and S. Kabir, *J. Phys.: Condens. Matter*, 2001, **13**, 641.
41 K. Kobayashi and K. Yamamoto, *J. Phys. Soc. Jpn.*, 2001, **70**, 1861.
42 L. L. Sun, T. Kikegawa, Q. Wu, Z. J. Zhan and W. K. Wang, *Chin. Phys. Lett.*, 2001, **18**, 1401.
43 J. M. An and W. E. Pickett, *Phys. Rev. Lett.*, 2001, **86**, 4366.
44 P. P. Singh, *Phys. Rev. Lett.*, 2001, **87**, 87004.
45 G. Satta, G. Profetta, F. Bernardini, A. Continenza and S. Masidda, *Phys. Rev. B*, 2001, **6410**, 4507.
46 N. I. Medvedeva, A. L. Ivanovskii, J. E. Medvedeva and A. J. Freeman, *Phys. Rev. B*, 2001, **64**, 020502.
47 S. Y. Zhang, J. Zhang, T. Y. Zhao, C. B. Rong, B. G. Shen and Z. H. Cheng, *Chin. Phys.*, 2001, **10**, 335.
48 T. Takenobu, T. Ito, D. H. Chi, K. Prassides and I. Iwasa, *Phys. Rev. Lett.*, 2001, **6413**, 4513.
49 M. J. Mehl, D. A. Papaconstantinopoulos and D. J. Singh, *Phys. Rev. B*, 2001, **6414**, 509.
50 S. Suzuki, S. Higai and K. Nakao, *J. Phys. Soc. Jpn.*, 2001, **70**, 1206.
51 J. S. Slusky, N. Rogado, K. A. Regan, M. A. Hayward, P. Khalifah, T. He, K. Inamaru, S. M. Loureiro, M. K. Haas, H. W. Zanderbergen and R. J. Cava, *Nature*, 2001, **410**, 343.
52 X. L. Chen, Q. Y. Tu, M. He, L. Dai and L. Wu, *J. Phys.: Condens. Matter*, 2001, **13**, 723.
53 V. A. Gasparov, N. S. Sidorov, I. I. Zver'kova and M. P. Kulakov, *JETP Lett.*, 2001, **73**, 532.
54 I. Felner, *Physica C*, 2001, **353**, 11.
55 Y. G. Zhao, X. P. Zhang, P. T. Qiao, S. L. Jia, B. S. Cao, M. H. Zhu, Z. H. Hzu, X. L. Wang and B. L. Gu, *Physica C*, 2001, **361**, 91.
56 Y. Zhao, Y. Feng, C. H. Cheng, L. Zhou, Y. Wu, T. Machi, Y. Fudamoto, N. Koshizuka and M. Murakami, *Appl. Phys. Lett.*, 2001, **79**, 1154.
57 S. M. Kazakov, M. Angst, J. Karpinski, I. M. Fita and R. Puzniak, *Solid State Commun.*, 2001, **119**, 1.
58 S. Xu, Y. Moritomo, K. Kato and A. Nakamura, *J. Phys. Soc. Jpn.*, 2001, **70**, 1889.
59 M. V. Indenbom, L. S. Uspenskaya, M. P. Kulakov, I. K. Bdikin and S. A. Zver'kov, *JETP Lett.*, 2001, **74**, 274.
60 A. E. Kar'kin, V. I. Voronin, T. V. D'yachkova, N. I. Kadyrova, A. P. Tyutyunik, V. G. Zubkov, Y. G. Zainulin, M. V. Sadovskii and B. N. Goshchitskii, *JETP Lett.*, 2001, **73**, 570.
61 C. Kloc, P. G. Simkins, T. Siegrist and R. A. Laudise, *J. Cryst. Growth*, 1997, **182**, 416.
62 A. F. Hebard, M. J. Rosseinsky, R. C. Haddon, D. W. Murphy, S. H. Glarum, T. T. M. Palstra, A. P. Ramirez and A. R. Kortan, *Nature*, 1991, **350**, 600.
63 J. Lu, L. Zhang, X. Zhang and X. Zhao, *Acta Mater. Compos. Sin.*, 1999, **16**, 1.
64 J. Hirosawa, S. Suzuki and K. Nakao, *Syn. Met.*, 2001, **121**, 1133.
65 V. Buntar, C. Krutzler, F. M. Sauerzopf, H. W. Weber, M. Haluska and H. Kuzmany, in *Recent Advances in the Chemistry and Physics of Fullerenes and Related Materials*, ed. P. V. Kamat, D. M. Guldi and K. M. Kadish, Electrochemical Society, Pennington, NJ, 1999, vol. 7, p. 99.
66 N. Sakamoto, T. Muranaka, T. Akune, M. Baenita and K. Luders, in *Advances in Superconductivity XI*, ed. N. Koshizuka and S. Tajima, Springer-Verlag, Tokyo, 1999, vol. 1, p. 629.
67 M. S. Fuhrer, K. Cherrey, A. Zettle, M. L. Cohen and V. H. Crespi, *Phys. Rev. Lett.*, 1999, **83**, 404.
68 J. H. Schön, C. Kloc, T. Siegrist, M. Steigerwald, C. Svensson and B. Batlogg, *Nature*, 2001, **413**, 831.
69 P. Grant, *Nature*, 2001, **413**, 264.
70 E. Dagotto, *Science*, 2001, **293**, 2410.
71 L. Bauernfeind, W. Widder and H. F. Braun, *Physica C*, 1995, **254**, 151.
72 I. Felner, U. Asaf, Y. Levi and O. Millo, *Phys. Rev. B*, 1997, **55**, 3374.

73 I. Felner and U. Asaf, *Superlattices Microstructures*, 1998, **24**, 99.
74 G. V. M. Williams and S. Krämer, *Phys. Rev. B*, 2000, **62**, 4132.
75 J. L. Tallon, C. Bernhard and J. W. Loram, *J. Low Temp. Phys.*, 1999, **117**, 825.
76 J. L. Tallon, J. W. Loram, G. V. M. Williams and C. Bernhard, *Phys. Rev. B*, 2000, **61**, 6471.
77 C. Bernhard, J. L. Tallon, C. Niedermayer, T. Blasius, A. Golnik, E. Brucher, R. K. Kremer, D. R. Noakes, C. E. Stronach and E. J. Ansaldo, *Phys. Rev. B*, 1999, **59**, 14099.
78 D. P. Hai, S. Kamisawa, I. Kakeya, M. Furuyama, T. Mochiku and K. Kadowaki, *Physica C*, 2001, **357–360**, 406.
79 Y. Tokunaga, H. Kotegawa, K. Ishida, Y. Kitaoka, H. Takagiwas and J. Akimitsu, *Phys. Rev. Lett.*, 2001, **86**, 5767.
80 V. P. S. Awana, J. Nakamura, M. Karppinen, H. Yamauchi, S. K. Malik and W. B. Yelon, *Physica C*, 2001, **357–360**, 121.
81 H. A. Blackstead, J. D. Dow, D. R. Harshman, W. B. Yelon, M. X. Chen, M. K. Wu, D. Y. Chen, F. Z. Chien and D. B. Pulling, *Phys. Rev. B*, 2001, **63**, 214412.
82 G. M. Kuz'micheva, V. V. Luparev, E. P. Khlybov, I. E. Kostleya, A. S. Andreenko and K. N. Gavrilov, *Physica C*, 2001, **350**, 105.
83 C. S. Knee, B. D. Rainford and M. T. Weller, *J. Mater. Chem.*, 2000, **10**, 2445.
84 I. Felner, U. Asaf, C. Godart and E. Alleno, *Physica C*, 1999, **259–261**, 703.
85 I. Felner and U. Asaf, *Physica C*, 1997, **292**, 97.
86 I. Felner, U. Asaf, F. Ritter, P. W. Klamut and B. Dabrowski, *Physica C*, 2001, **364–365**, 368.
87 I. Felner and U. Asaf, *Physica C*, 1997, **292**, 97.
88 I. Felner, *Hyperfine Interactions*, 1998, **113**, 477.
89 E. B. Sonin and I. Felner, *Phys. Rev. B*, 1998, **57**, 14000.
90 E. B. Sonin, *J. Low Temp. Phys.*, 1998, **110**, 411.
91 I. Felner, E. B. Sonin, T. Machi and N. Koshizuka, *Physica C*, 2000, **341–348**, 715.
92 X. H. Chen, Z. Sun, K. Q. Wang, Y. M. Xiong, H. S. Yang, H. H. Wen, Y. M. Nis and Z. X. Zhao, *J. Phys.: Condens. Matter*, 2000, **12**, 10561.
93 I. Matsubara, N. Kida, R. Funahashi, K. Ueno and N. Ohno, in *Proceedings of the 10th International Symposium on Superconductivity, 1997, Gifu, Japan*, ed. K. Osamura and I. Hirabayashi, Springer-Verlag, Tokyo, 1998, p. 297.
94 J. Tallon, C. Bernhard, M. Bowden, P. Gilberd and T. Stoto, *IEEE Trans. Appl. Supercond.*, 1999, **9**, 1696.
95 C. T. Lin, B. Liang, C. Ulrich and C. Bernhard, *Physica C*, 2001, **364–365**, 373.
96 J. E. McCrone, G. Gibson, J. L. Tallon, J. R. Cooper and Z. Barber *Proceedings of the 12th International Symposium on Superconductivity, (ISS'99), 1999, Morioka, Japan*, ed. T. Yamashita, K. Tanabe, Springer-Verlag, Tokyo, 2000, p. 80.
97 (*a*) C. W. Chu, Y. Y. Xue, Y. S. Wang, A. K. Heilman, B. Lorenz, R. L. Meng, J. Cmaidalka and L. M. Dezaneti, *J. Supercond.*, 2000, **13**, 679; (*b*) C. W. Chu, *Physica C*, 2000, **341–348**, 25.
98 Y. Y. Xue, R. L. Meng, J. Cmaidalka, B. Lorenz, L. M. Desaneti, A. K. Heilman and C. W. Chu, *Physica C*, 2000, **341–348**, 459.
99 C. Bernhard, J. L. Tallon, E. Brucher and R. K. Kremer, *Phys. Rev. B*, 2000, **61**, 14960.
100 Y. Y. Xue, S. Tsui, J. Cmaidalka, R. L. Meng, B. Lorenz and C. W. Chu, *Physica C*, 2000, **341–348**, 483.
101 A. C. McLaughlin, W. Zhou, J. P. Atfield, A. N. Fitch and J. L Tallon, *Phys. Rev. B*, 1999, **60**, 7512.
102 K. Otzschi, T. Mizukami, T. Hinouchi, J. Shimoyama and K. Kishio, *J. Low Temp. Phys.*, 1999, **117**, 855.
103 R. W. Henn, H. Friedrich, V. P. S. Awana and E. Gmelin, *Physica C*, 2000, **341–348**, 457.
104 Z. Sun, S. Y. Li, Y. M. Xiong and X. H. Chen, *Physica C*, 2001, **349**, 289.
105 P. W. Klamut, B. Dabrowski, S. M. Mini, S. Kolesnik, J. Mais, A. Shengelaya, R. Khasano, I. Savic, H. Keller, T. Graber, J. Gebhardt, P. J. Viccaro and Y. Xiao, *Physica C*, 2001, **364**, 313.
106 A. C. McLaughlin and J. P. Attfield, *Phys. Rev. B*, 1999, **60**, 14605.
107 A. C. McLaughlin, V. Janowitz, J. A. McAllister and J. P. Attfield, *Chem. Commun.*, 2000, **14**, 1331.
108 A. C. McLaughlin, Y. Janowitz, J. A. McAllister and J. P. Attfield, *J. Mater. Chem.*, 2001, **11**, 173.
109 J. T. Rijssenbeek, N. Mansourian-Hadavi, S. Malo, D. Ko, C. Washburn, A. Maignan, D. Pelloquin, T. O. Mason and K. R. Poeppelmeier, *Physica C*, 2000, **341–348**, 481.
110 M. B. Feng, M. H. Fang, Z. Xu and Z. K. Jiao, *Chin. Phys. Lett.*, 2001, **18**, 963.
111 P. W. Klamut, B. Dabrowski, S. Kolesnik, M. Maxwell and J. Mais, *Phys. Rev. B*, 2001, **63**, 224512.
112 A. V. Boris, P. Mandal, C. Bernhard, N. N. Kovaleva, K. Pucher, J. Hemberger and A. Loidl, *Phys. Rev. B*, 2001, **63**, 18505.
113 H. A. Blackstead, J. D. Dow, D. R. Harshman, D. B. Pulling, Z. F. Ren and D. Z. Wang, *Physica C*, 2001, **364**, 305.
114 Y. Furukawa, S. Takada, A. Yamanaka and K. Kumagai, *Physica C*, 2000, **341–348**, 453.
115 A. Butera, A. Fainstein, E. Winkler and J. Tallon, *Phys. Rev. B*, 2001, **63**, 54442.
116 A. Butera, A. Fainstein, E. Winkler, J. van Tol, S. B. Oseroff and J. Tallon, *J. Appl. Phys.*, 2001, **89**, 7666.
117 K. Kumagai, S. Takada and Y. Furukawa, *Phys. Rev. B*, 2001, **63**, 180509.
118 H. Srikanth, L. Spinu, T. Kodendandath, J. B. Wiley and J. Tallon, *J. Appl. Phys.*, 2001, **89**, 7487.

119 A. Fainstein, E. Winkler, A. Butera and J. Tallon, *Phys. Rev. B*, 1999, **60**, 12597.
120 J. E. McCrone, J. R. Cooper and J. L. Tallon, *J. Low Temp. Phys.*, 1999, **117**, 1199.
121 R. Weht, A. B. Schick and W. E. Pickett, *Am. Inst. Phys. Conf. Proc.*, 1999, **483**, 141.
122 J. X. Zhu, C. S. Ting and C. W. Chu, *Phys. Rev. B*, 2000, **62**, 11369.
123 K. Nakamura, K. T. Park, A. J. Freeman and J. D. Jorgensen, *Phys. Rev. B*, 2001, **63**, 24507.
124 H. Shimahara and S. Hara, *Phys. Rev. B*, 2000, **62**, 14541.
125 A. B. Shick, R. Weht and W. E. Pickett, *J. Supercond.*, 2000, **13**, 687.
126 W. E. Pickett, R. Weht and A. B. Shick, *Phys. Rev. Lett.*, 1999, **83**, 3713.
127 Y. Kanegae and Y. Ohashi, *J. Phys. Soc. Jpn.*, 2001, **70**, 2124.
128 M. Houzet, A. Buzdin and M. L. Kulic, *Phys. Rev. B*, 2001, **64**, 184501.
129 E. V. Kuz'min, S. G. Ovchinnikov, I. O. Baklanov and E. G. Goryachev, *Zh. Eksp. Teor. Fiz.*, 2000, **118**, 404.
130 D. Y. Chen, F. Z. Chien, D. C. Ling, J. L. Tseng, S. R. Sheen, M. J. Wang and M. K. Wu, *Physica C*, 1997, **282–287**, 73.
131 M. K. Wu, D. Y. Chen, F. Z. Chien, S. R. Sheen, D. C. Ling, C. Y. Tai, G. Y. Tseng, D. H. Chen and F. C. Zhang, *Z. Phys. B*, 1997, **102**, 37.
132 M. K. Wu, D. Y. Chen, F. Z. Chien, D. C. Ling, Y. Y. Chen and H. C. Ren, *Int. J. Mod. Phys. B*, 1999, **13**, 3585.
133 H. Blackstead, J. D. Dow, P. J. McGinn and D. B. Pulling, *J. Supercond.*, 2000, **13**, 977.
134 H. A. Blackstead, J. D. Dow, D. R. Harshman, M. J. DeMarco, M. K. Wu, D. Y. Chen, F. Z. Chien, D. B. Pulling, W. J. Kossler, A. J. Greer, C. E. Stronach, E. Koster, B. Hitti, M. Haka and S. Toorongian, *Eur. Phys. J. B*, 2000, **15**, 649.
135 M. K. Wu, D. Y. Chen, D. C. Ling and F. Z. Chien, *Physica B*, 2000, **284**, 477.
136 H. A. Blackstead, J. D. Dow and D. R. Harshmann, *J. Supercond.*, 2000, **13**, 981.
137 M. DeMarco, H. A. Blackstead, J. D. Dow, M. K. Wu, D. Y. Chen, F. Z. Chien, M. Haka, S. Toorongian and J. Fridmann, *Phys. Rev. B*, 2000, **62**, 14301.
138 H. A. Blackstead, J. D. Dow, D. R. Harshman, W. B. Yelon, M. X. Chen, M. K. Wu, D. Y. Chen, F. Z. Chien and D. B. Pulling, *Phys. Rev. B*, 2001, **63**, 214412.
139 D. R. Harshman, W. J. Kossler, A. J. Greer, C. E. Stronach, D. R. Noakes, E. Koster, M. K. Wu, F. Z. Chien, H. A. Blackstead, D. B. Pulling and J. D. Dow, *Physica C*, 2001, **364–365**, 392.
140 H. Yamamoto, M. Naito and H. Sato, *Physica C*, 2000, **338**, 29.
141 S. Karimoto, H. Yamamoto, T. Greibe and M. Naito, *Jpn. J. Appl. Phys.*, 2001, **40**, 127.
142 S. Karimoto and M. Naito, *Physica C*, 2000, **338**, 995.
143 S. Karimoto and M. Naito, *Physica B*, 2000, **284**, 1113.
144 E. G. Maksimov, *Usp. Fiz. Nauk*, 2000, **170**, 1033 (*Phys.–Uspekhi*, 2000, **43**, 965).
145 M. V. Sadovskii, *Usp. Fiz. Nauk*, 2001, **171**, 539 (*Phys.–Uspekhi*, 2001, **44**, 515).
146 M. Buchanan, *Nature*, 2001, **409**, 8.
147 B. Batlogg and C. Varma, *Phys. World*, 2000, **13**, 33.
148 D. G. Hinks, H. Claus and J. D. Jorgensen, *Nature*, 2001, **411**, 457.
149 J. H. Schön, C. Kloc and B. Batlogg, *Science*, 2001, **293**, 2432.
150 J. G. Bednorz and K. A. Müller, *Z. Phys. B*, 1986, **64**, 189.
151 J. Vanacken, *Physica B*, 2001, **294–295**, 347.
152 T. Timusk and B. Statt, *Rep. Prog. Phys.*, 1999, **62**, 61.
153 R. W. Hill, C. Proust, L. Taillefer, P. Fournier and R. L. Green, *Nature*, 2001, **414**, 711.
154 J. L. Tallon and J. W. Loram, *Physica C*, 2001, **349**, 53.
155 A. Leridon, A. Défossez, J. Dumont, J. Lesueur and J. P. Contour, *Phys. Rev. Lett.*, 2001, **87**, 197007.
156 V. V. Moshchalkov, J. Vanacken and L. Trappeniers, *Phys. Rev. B*, 2001, **64**, 214504.
157 J. L. Tallon, J. W. Loram, G. V. M. Williams, J. R. Cooper, I. R. Fisher, J. D. Johnson, M. P. Staines and C. Bernhard, *Phys. Status Solidi B*, 1999, **215**, 531.
158 V. Emery and S. A. Kivelson, *Nature*, 1995, **374**, 434.
159 V. B. Geshkenbein, L. B. Ioffe and A. I. Larkin, *Phys. Rev. B*, 1997, **55**, 3173.
160 V. P. Gusynin, V. M. Loktev and S. G. Sharapov, *J. Exp. Theoret. Phys.*, 1999, **88**, 685.
161 B. Jankó, J. Maly and K. Levin, *Phys. Rev. B*, 1997, **56**, 11407.
162 J. Maly, B. Jankó and K. Levin, *Phys. Rev. B*, 1999, **59**, 1354.
163 Q. J. Chen, I. Kosztin, B. Jankó and K. Levin, *Phys. Rev. Lett.*, 1998, **81**, 4708.
164 Q. Chen, K. Levin and I. Kosztin, *Phys. Rev. B*, 2001, **63**, 184519.
165 M. Randeria, in *Models and Phenomenology for Conventional and High-Temperature Superconductivity*, ed. G. Iadonisi, J. R. Schrieffer and M. L. Chiofalo, IOS Press, Amsterdam, 1999.
166 D. Pines, *Physica C*, 2000, **341**, 59.
167 J. Schmaian, D. Pines and B. Stojkovic, *Phys. Rev. Lett.*, 1998, **80**, 3839.
168 J. Schmaian, D. Pines and B. Stojkovic, *Phys. Rev. B*, 1999, **60**, 667.
169 E. Z. Kuchinskii and M. V. Sadovskii, *J. Exp. Theoret. Phys.*, 1999, **88**, 968.
170 C. Castellani, C. D. Castro, M. Grilli and A. Perali, *Physica C*, 2000, **341–348**, 1739.
171 D. Daghero, R. S. Gonnelli, A. Morello, G. A. Ummarino, L. Natale, V. A. Stepanov, F. Licci and G. Ubertalli, *Int. J. Modern Phys. B*, 2000, **14**, 2779.

172 S. Sachdev, in *Proceedings of the International Summer School on Fundamental Problems in Statistical Physics, August–September 2001, Altenberg, Germany*, ed. H. van Beijeen, to be published in *Physica A*, available at cond-mat/0109419.
173 G. Deutscher, *Nature*, 1999, **397**, 410.
174 Z. A. Xu, N. P. Ong, Y. Wang, T. Kakeshita and S. Uchida, *Nature*, 2000, **406**, 486.
175 A. A. Abrikosov, *Phys. Rev. B*, 2001, **63**, 134518.
176 A. A. Abrikosov, *Physica C*, 1999, **317–318**, 154.
177 A. A. Varlamov, G. Balestrino, E. Milani and D. V. Livanov, *Adv. Phys.*, 1999, **48**, 655.
178 V. M. Krasnov, A. Yurgens, D. Winkler, P. Delsing and T. Claeson, *Phys. Rev. Lett.*, 2000, **84**, 5860.
179 V. M. Krasnov, A. E. Kovalev, A. Yurgens and D. Winkler, *Phys. Rev. Lett.*, 2001, **86**, 2657.
180 K. Gorny, O. M. Vyaselev, J. A. Martindale, V. A. Nandor and C. H. Pennington, *Phys. Rev. Lett.*, 1999, **82**, 177.
181 G. Q. Zheng, W. G. Clark, Y. Kitaoka, K. Asayama, Y. Kodama, P. Kuhns and W. G. Moulton, *Phys. Rev. B*, 1999, **60**, 9947.
182 G. Q. Zheng, H. Ozaki, W. G. Clark, Y. Kitaoka, P. Kuhns, A. P. Reyes, W. G. Moulton, T. Kondo, Y. Shimakawa and Y. Kubo, *Phys. Rev. Lett.*, 2000, **85**, 405.
183 V. F. Mitrovic, H. N. Bachman, W. P. Halperin, M. Eschrig, J. A. Sauls, A. P. Reyes, P. Kuhns and W. G. Moulton, *Phys. Rev. Lett.*, 1999, **82**, 2784, and references therein.
184 T. Shibauchi, L. Krusin-Elbaum, M. Li, M. P. Maley and P. H. Kes, *Phys. Rev. Lett.*, 2001, **86**, 5763.
185 T. Startseva, T. Timusk, A. V. Puchkov, D. N. Basov, H. A. Mook, M. Okuya, T. Kimura and K. Kishio, *Phys. Rev. B*, 1999, **59**, 7184.
186 E. J. Singley, D. N. Basov, K. Kurahashi, T. Uefuji and K. Yamada, *Phys. Rev. B*, 2001, **64**, 224503.
187 T. Tohyama and S. Maekawa, *Supercond. Sci. Technol.*, 2000, **13**, R17.
188 See, for example, M. R. Norman, H. Ding, M. Randeria, J. C. Campuzano, T. Yokoya, T. Takeuchi, T. Takahashi, T. Mochiku, K. Kadowaki, P. Guptasarma and D. G. Hinks, *Nature*, 1998, **392**, 157.
189 C. C. Tsuei and J. R. Kirtley, *Rev. Mod. Phys.*, 2000, **72**, 969.
190 S. V. Borisenko, A. A. Kordyuk, S. Legner, C. Durr, M. Knupfer, M. S. Golden, J. Fink, K. Nenkov, D. Eckert, G. Yang, S. Abell, H. Berger, L. Forro, B. Liang, A. Maljuk, C. T. Lin and H. B. Keimer, *Phys. Rev. B*, 2001, **64**, 094513.
191 N. L. Saini, J. Avila, A. Bianconi, A. Lanzara, M. C. Asensio, S. Tajima, G. D. Gu and N. Koshizuka, *Phys. Rev. Lett.*, 1997, **79**, 3467.
192 Y. D. Chuang, A. D. Gromko, D. S. Dessau, Y. Aiura, Y. Yamaguchi, K. Oka, A. J. Arko, J. Joyce, H. Eisaki, S. I. Uchida, K. Nakamura and Y. Ando, *Phys. Rev. Lett.*, 1999, **83**, 3717.
193 D. L. Feng, W. J. Zheng, K. M. Shen, D. H. Lu, F. Ronning, J. I. Shimoyama, K. Kishio, G. Gu, D. Van der Marel, Z. X. Shen, submitted to *Phys. Rev. Lett.*, available at cond-mat/9908056.
194 S. V. Borisenko, M. S. Golden, S. Legner, T. Pichler, C. Durr, M. Knupfer, J. Fink, G. Yang, S. Abell and H. Berger, *Phys. Rev. Lett.*, 2000, **84**, 4453.
195 H. M. Fretwell, A. Kaminski, J. Mesot, J. C. Campuzano, M. R. Norman, M. Randeria, T. Sato, R. Gatt, T. Takahashi and K. Kadowaki, *Phys. Rev. Lett.*, 2000, **84**, 4449.
196 C. C. Tsuei and J. R. Kirtley, *Phys. Rev. Lett.*, 2000, **85**, 182.
197 P. W. Anderson, *The Theory of Superconductivity in the High-T_c* Cuprates, Princeton University Press, 1997.
198 P. W. Anderson, in *High-Temperature Superconductivity*, AIP Conference Proceedings, vol.483, ed. S. E. Barnes, J. Ashkenazi, J. Cohn and F. Zuo, American Institute of Physics, Woodbury, New York, 1999, p. 3.
199 P. W. Anderson, *Science*, 1987, **235**, 1136.
200 S. Spielman, K. Fesler, C. B. Eom, T. H. Geballe, M. M. Fejer and A. Kapitulnik, *Phys. Rev. Lett.*, 1990, **65**, 123.
201 P. L. Gammel, P. A. Polakos, C. E. Rice, L. R. Harriott and D. J. Bishop, *Phys. Rev. B*, 1990, **41**, 2593.
202 M. R. Norman, *J. Phys. Chem. Solids*, 1993, **54**, 1165.
203 A. Leggett, *Phys. World*, 1997, **10**, 51.
204 S. L. Bud'ko, G. Lapertot, C. Petrovic, C. E. Cunningham, N. Anderson and P. C. Canfield, *Phys. Rev. Lett.*, 2001, **86**, 1877.
205 F. Marsiglio, *Phys. Rev. Lett.*, 2001, **87**, 247001.
206 R. A. Kaindl, M. A. Carnahan, J. Orenstein, D. S. Chemla, H. M. Christen, H. Y. Zhai, M. Paranthaman and D. H. Lowndes, *Phys. Rev. Lett.*, 2002, **88**, 027003.
207 Y. Kong, O. V. Dolgov, O. Jepsen and O. K. Andersen, *Phys. Rev. B*, 2001, **64**, 020501.
208 J. Kortus, I. I. Mazin, K. D. Belashchenko, V. P. Antropov and L. L. Boyer, *Phys. Rev. Lett.*, 2001, **86**, 4656.
209 A. Y. Liu, I. J. Mazin and J. Kortus, *Phys. Rev. Lett.*, 2001, **87**, 087005.
210 J. E. Hirsch, *Phys. Lett. A*, 2001, **282**, 392.
211 J. E. Hirsch and F. Marsiglio, *Phys. Rev. B*, 2001, **64**, 144523.
212 A. S. Alexandrov, *Physica C*, 2001, **363**, 231.
213 E. Cappelluti, S. Ciuchi, E. Grimaldi, L. Pietronero and S. Strässler, *Phys. Rev. Lett.*, 2002, **88**, 117003.

214 J. E. Hirsch, to be published in *Studies of High Temperature Superconductivity*, ed. A. Narlikar, Nova Science Publishers, Commack, NY.
215 Y. X. Wang, T. Plackowski and A. Junod, *Physica C*, 2001, **355**, 179.
216 S. Tsuda, T. Yokoya, T. Kiss, Y. Takano, K. Togano, H. Kito, H. Ihara and S. Shin, *Phys. Rev. Lett.*, 2001, **87**, 177006.
217 F. Giubileo, D. Roditchev, W. Sacks, R. Lamy, D. X. Thanh, J. Klein, S. Miraglia, D. Fruchart, J. Marcus and P. Monod, *Phys. Rev. Lett.*, 2001, **87**, 177008.
218 F. Laube, G. Goll, J. Hagel, H. von Hohneysen and T. Wolf, *Europhys. Lett.*, 2001, **56**, 296.
219 K. D. Belashchenko, M. van Schilfgarde and V. P. Antropov, *Phys. Rev. B*, 2001, **64**, 092503.
220 S. Ohshima, T. Koseki and A. Kamimura, *Jpn. J. Appl. Phys.*, 1998, **37**, 375.
221 A. Tonomura, H. Kasai, O. Kamimura, T. Matsuda, K. Harada, Y. Nakayama, J. Shimoyama, K. Kishio, T. Hanaguri, K. Kitazawa, M. Sasase and S. Okayasu, *Nature*, 2001, **412**, 620.
222 S. L. Lee, C. M. Aegerter, S. H. Lloyd, E. M. Forgan, C. Ager, M. B. Hunt, H. Keller, I. M. Savic, R. Cubitt, G. Wirth, K. Kadowaki and N. Koshizuka, *Phys. Rev. Lett.*, 1998, **81**, 5209.
223 W. K. Kwok, R. J. Olsson, G. Karapetrov, L. M. Paulius, W. G. Moulton, D. J. Hofman and G. W. Crabtree, *Phys. Rev. Lett.*, 2000, **84**, 3706.
224 P. Sen, N. Trivedi and D. M. Ceperley, *Phys. Rev. Lett.*, 2001, **86**, 4092.
225 C. J. van der Beek, M. Konczykowski, A. V. Samoilov, N. Chikumoto, S. Bouffard and M. V. Feigel'man, *Phys. Rev. Lett.*, 2001, **86**, 5136.
226 K. Itaka, T. Shibauchi, M. Yasugaki, T. Tamegai and S. Okayasu, *Phys. Rev. Lett.*, 2001, **86**, 5144.
227 N. Morozov, M. P. Maley, L. N. Bulaevskii, V. Thorsmølle, A. E. Koshelev, A. Petrean and W. K. Kwok, *Phys. Rev. Lett.*, 1999, **82**, 1008.
228 M. V. Indenbom, C. J. van der Beek, M. Konczykowski and F. Holtzberg, *Phys. Rev. Lett.*, 2000, **84**, 1972.
229 B. Dam, J. M. Huijbregtse, F. C. Klaassen, R. C. F. van der Geest, G. Doornbos, J. H. Rector, A. M. Testa, S. Freisem, J. C. Martinezk, B. Stäuble-Pümpin and R. Griessen, *Nature*, 1999, **399**, 439.
230 V. M. Pan and A. V. Pan, *Low Temp. Phys.*, 2001, **27**, 732 (*Fiz. Niz. Temp.*, 2001, **27**, 991).
231 F. C. Klaassen, G. Doornbos, J. M. Huijbregtse, R. C. F. van der Geest, B. Dam and R. Griessen, *Phys. Rev. B*, 2001, **64**, 184523.
232 A. Diaz, L. Mechin, P. Berghuis and J. E. Evetts, *Phys. Rev. Lett.*, 1998, **80**, 3855.
233 Ch. Jooss, R. Warthmann, H. Kronmüller, T. Haage, H. U. Habermeier and J. Zegenhagen, *Phys. Rev. Lett.*, 1999, **82**, 632.
234 H. Safar, S. Foltyn, H. Kung, M. P. Maley, J. O. Willis, P. Arendt and X. D. Wu, *Appl. Phys. Lett.*, 1996, **68**, 1853.
235 A. Casaca, G. Bonfait, M. Getta, M. Lenkens and G. Muller, *Phys. Rev. B*, 1999, **59**, 1538.
236 C. Villard, G. Koren, D. Cohen, E. Polturak, B. Thrane and D. Chateignier, *Phys. Rev. Lett.*, 1996, **77**, 3913.
237 H. Yamasaki, A. Rastogi and A. Sawa, *Physica C*, 2000, **335**, 175.
238 Y. Paltiel, E. Zeldov, Y. Myasoedov, M. L. Rappaport, G. Jung, S. Bhattacharya, M. J. Higgins, Z. L. Xiao, E. Y. Andrei, P. L. Gammel and D. J. Bishop, *Phys. Rev. Lett.*, 2000, **85**, 3712.
239 C. J. van der Beek, S. Colson, M. V. Indenbom and M. Konczykowski, *Phys. Rev. Lett*, 2000, **84**, 4196.
240 Y. Paltiel, E. Zeldov, Y. Myasoedov, H. Shtrikman, S. Bhattacharya, M. J. Higgins, Z. L. Xiao, E. Y. Andrei, P. L. Gammel and D. J. Bishop, *Nature*, 2000, **403**, 398.
241 M. Marchevsky, M. J. Higgins and S. Bhattacharya, *Nature*, 2001, **409**, 591.
242 T. Nishizaki, T. Naito, S. Okayasu, A. Iwase and N. Kobayashi, *Phys. Rev. B*, 2000, **61**, 3649.
243 G. P. Mikitik and E. H. Brandt, *Phys. Rev. B*, 2001, **64**, 184514.
244 S. Kokkaliaris, P. A. J. de Groot, S. N. Gordeev, A. A. Zhukov, R. Gagnon and L. Taillefer, *Phys. Rev. Lett.*, 1999, **82**, 5116.
245 S. Kokkaliaris, A. A. Zhukov, P. A. J. de Groot, R. Gagnon, L. Taillefer and T. Wolf, *Phys. Rev. B*, 2000, **61**, 3655.
246 X. S. Ling, S. R. Park, B. A. McClain, S. M. Choi, D. C. Dender and J. W. Lynn, *Phys. Rev. Lett.*, 2001, **86**, 712.
247 A. van Otterlo, R. T. Scalettar, G. T. Zimanyi, R. Olsson, A. Petrean, W. Kwok and V. Vinokur, *Phys. Rev. Lett.*, 2000, **84**, 2493.
248 V. F. Correa, G. Nieva and F. de la Cruz, *Phys. Rev. Lett.*, 2001, **87**, 057003.
249 P. Esquinazi, R. Höhne, Y. Kopelevich, A. V. Pan and M. Ziese, in *Physics and Materials Science of Vortex States, Flux Pinning and Dynamics*, ed. R. Kossowsky, S. Bose, V. Pan and Z. Durusoy, Kluwer, Dordrecht, 1999, p. 149.
250 D. Dominguez, *Phys. Rev. Lett.*, 1999, **82**, 181.
251 C. J. Olson, C. Reichhardt and F. Nori, *Phys. Rev. Lett.*, 1998, **81**, 3757.
252 C. J. Olson, G. T. Zimányi, A. B. Kolton and N. Grønbech-Jensen, *Phys. Rev. Lett.*, 2000, **85**, 5416.
253 A. V. Pan and P. Esquinazi, *Eur. Phys. J. B*, 2000, **17**, 405.
254 A. V. Pan and P. Esquinazi, *Physica C*, 2000, **341**, 1187.
255 Y. Soibel, Y. Myasoedov, M. L. Rappaport, T. Tamegai, S. S. Banerjee and E. Zeldov, *Phys. Rev. Lett.*, 2001, **87**, 167001.

256 N. Avraham, B. Khaykovich, Y. Myasoedov, M. Rappaport, H. Shtrikman, D. E. Feldman, T. Tamegai, P. H. Kes, M. Li, M. Konczykowski, K. van der Beek and E. Zeldov, *Nature*, 2001, **411**, 451.
257 M. J. Qin, X. L. Wang, S. Soltanian, A. H. Li, H. K. Liu and S. X. Dou, *Phys. Rev. B*, 2001, **64**, 060505; M. J. Qin, X. L. Wang, H. K. Liu and S. X. Dou, *Phys. Rev. B*, 2002, **65**, 132508.
258 S. O. Valenzuela and V. Bekeris, *Phys. Rev. Lett.*, 2000, **84**, 4200.
259 S. O. Valenzuela and V. Bekeris, *Phys. Rev. Lett*, 2001, **86**, 504.
260 J. J. Akerman, S. H. Yun, U. O. Karlsson and K. V. Rao, *Phys. Rev. B*, 2001, **64**, 024526.
261 G. Pasquini, L. Civale, H. Lanza and G. Nieva, *Phys. Rev. B*, 1999, **59**, 9627.
262 J. J. Akerman, E. L. Venturini, M. P. Siegal, S. H. Yun, U. O. Karlsson and K. V. Rao, *Phys. Rev. B*, 2001, **64**, 094509.
263 M. J. Qin and C. K. Ong, *Phys. Rev. B*, 2000, **61**, 9786.
264 M. J. Qin and C. K. Ong, *Physica C*, 2000, **334**, 107.
265 A. V. Pan, F. Ciovacco, P. Equinazi and M. Lorenz, *Phys. Rev. B*, 1999, **60**, 4293.
266 M. Ziese, *Phys. Rev. B*, 1996, **53**, 12422.
267 M. Ziese, *Physica C*, 1996, **269**, 35.
268 M. Ziese, *Phys. Rev. B*, 1997, **55**, 8106.
269 E. H. Brandt, *Phys. Rev. B*, 1998, **58**, 6506.
270 E. H. Brandt, *Phys. Rev. B*, 1998, **58**, 6523.
271 E. H. Brandt, *Phys. Rev. B*, 1999, **60**, 11939.
272 E. H. Brandt, *Phys. Rev. B*, 1999, **59**, 3369.
273 E. H. Brandt and G. P. Mikitik, *Phys. Rev. Lett.*, 2000, **85**, 4164.
274 M. J. Qin and C. J. Ong, *Physica C*, 1999, **325**, 107.
275 G. P. Mikitik and E. H. Brandt, *Phys. Rev. B*, 2000, **62**, 6800.
276 G. P. Mikitik and E. H. Brandt, *Phys. Rev. B*, 2000, **62**, 6812.
277 M. H. Jung, M. Jaime, A. H. Lacerda, G. S. Boebinger, W. N. Kang, H. J. Kim, E. M. Choi and S. I. Lee, *Chem. Phys. Lett.*, 2001, **343**, 447.
278 S. Patnaik, L. D. Cooley, A. Gurevich, A. A. Polyanskii, J. Jing, X. Y. Cai, A. A. Squitteri, M. T. Naus, M. K. Lee, J. H. Choi, L. Belenky, S. D. Bu, J. Letteri, X. Song, D. G. Schlom, S. E. Babcock, C. B. Eom, E. E. Hellstrom and D. C. Larbalestier, *Supercond. Sci. Technol.*, 2001, **14**, 315.
279 O. F. de Lima, R. A. Ribeiro, M. A. Avila, C. A. Cardoso and A. A. Coelho, *Phys. Rev. Lett.*, 2001, **86**, 5974.
280 O. F. de Lima, C. A. Cardoso, R. A. Ribeiro, M. A. Avila and A. A. Coelho, *Phys. Rev. B*, 2001, **6414**, 4517.
281 F. Simon, A. Janossy, T. Feher, F. Muranyi, S. Garaj, L. Forro, C. Petrovic, S. L. Bud'ko, G. Lapertot, V. G. Kogan and P. C. Canfield, *Phys. Rev. Lett.*, 2001, **87**, 470021.
282 G. Fuchs, K. H. Muller, A. Handstein, K. Nenkov, V. N. Narozhnyi, D. Eckert, M. Wolf and L. Schultz, *Solid State Commun.*, 2001, **118**, 497.
283 S. L. Bud'ko, C. Petrovic, G. Lapertot, C. E. Cunningham, P. C. Canfield, M. H. Jung and A. H. Lacerda, *Phys. Rev. B*, 2001, **63**, 220503.
284 K. H. Muller, G. Fuchs, A. Handstein, K. Nenkov, V. N. Narozhnyi and D. Eckert, *J. Alloys Compounds*, 2001, **322**, L10.
285 L. Wang, H. S. Lim and C. K. Ong, *Supercond. Sci. Technol.*, 2001, **14**, 754.
286 Y. Takano, H. Takeya, H. Fujii, H. Kumakura, T. Hatano, K. Togano, H. Kito and H. Ihara, *Appl. Phys. Lett.*, 2001, **78**, 2914.
287 A. G. Joshi, C. G. S. Pillai, P. Raj and S. K. Mallik, *Solid State Commun.*, 2001, **118**, 445.
288 M. K. Bhide, R. M. Kadam, M. D. Sastry, A. Singh, S. Sen, D. K. Aswal, S. K. Gupta and V. C. Sahni, *Supercond. Sci. Technol.*, 2001, **14**, 572.
289 S. L. Li, H. H. Wen, Z. W. Zhao, Y. M. Ni, Z. A. Ren, G. C. Che, H. P. Yang, Z. Y. Liu and Z. X. Zhao, *Phys. Rev. B*, 2001, **6409**, 4522.
290 H. Jin, H. H. Wen, S. L. Li, Z. W. Zhao, Y. M. Ni, Z. A. Ren, G. C. Che, H. P. Yang, Z. Y. Liu, D. N. Zheng and Z. X. Zhao, *Chin. Phys. Lett.*, 2001, **18**, 823.
291 G. Ghigo, D. Botta, A. Chiodoni, R. Gerbaldo, L. Gozzelini, E. Mezzetti, B. Minetti, S. Ceresara, G. Giunchi and G. Ripamonti, *Supercond. Sci. Technol.*, 2001, **14**, 722.
292 A. V. Pronin, A. Pimenov and S. I. Krasnosvobodtsev, *Phys. Rev. Lett.*, 2001, **87**, 970031.
293 C. Panagopoulos, B. D. Rainford, T. Xiang, C. A. Scott, M. Kambara and I. H. Inoue, *Phys. Rev. B*, 2001, **64**, 094514.
294 Y. Bugoslavsky, G. K. Perkins, X. Qi, L. F. Cohen and A. D. Caplin, *Nature*, 2001, **410**, 563.
295 Z. W. Zhao, H. H. Wen, S. L. Li, Y. M. Ni, Z. A. Ren, G. C. Che, H. P. Yang, Z. Y. Liu and Z. X. Zhao, *Chin. Phys.*, 2001, **10**, 340.
296 M. S. Kim, C. U. Jung, M. S. Park, S. Y. Lee, K. H. P. Kim, W. N. Kang and S. I. Lee, *Phys. Rev. B*, 2001, **64**, 012511.
297 H. H. Wen, S. L. Li, Z. W. Zhao, H. Jin, Y. M. Ni, W. N. Kang, H. J. Kim, E. M. Choi and S. I. Lee, *Phys. Rev. B*, 2001, **6413**, 4505.
298 Y. Bugoslavsky, L. F. Cohen, G. K. Perkins, M. Polichetti, T. J. Tate, R. Gwilliam and A. D. Caplin, *Nature*, 2001, **411**, 561.

299 E. Babic, B. Miljanic, K. Zadro, I. Kusevic, Z. Marohnic, D. Drobac, X. L. Wang and S. X. Dou, *Fizika A*, 2001, **10**, 87.
300 M. Eisterer, M. Zehetmayer, S. Tönies, H. W. Weber, M. Kambara, N. Hari Babu, D. A. Cardwell and L. R. Greenwood, *Supercond. Sci. Technol.*, 2002, **15**, 9.
301 R. J. Olsson, W. K. Kwok, G. Karapetrov, M. Iavarone, H. Claus, C. Peterson, G. W. Crabtree, W. N. Kang, H. J. Kim, E. M. Choi and S. I. Lee, to be published in the *Proceedings of the Annual American Physical Society March Meeting, Indianapolis, March 2002*, available at cond-mat/0201022.
302 H. H. Wen, S. L. Li, Z. W. Zhao, Y. M. Ni, Z. A. Ren, G. C. Che, H. P. Yang, Z. Y. Liu and Z. X. Zhao, *Chin. Phys. Lett.*, 2001, **18**, 816.
303 H. H. Wen, S. L. Li, Z. W. Zhao, H. Jin, Y. M. Ni, Z. A. Ren, G. C. Che and Z. X. Zhao, *Physica C*, 2001, **363**, 170.
304 T. H. Johansen, M. Baziljevich, D. V. Shantsev, P. E. Goa, Y. M. Galperin, W. N. Kang, H. J. Kim, E. M. Choi, M. S. Kim and S. I. Lee, *Supercond. Sci. Technol.*, 2001, **14**, 726.
305 A. A. Polyanskii, A. Gurevich, J. Jiang, D. C. Larbalestier, S. L. Bud'ko, D. K. Finnemore, G. Lapertot and P. C. Canfield, *Supercond. Sci. Technol.*, 2001, **14**, 811.
306 S. X. Dou, X. L. Wang, J. Horvat, D. Milliken, A. H. Li, K. Konstantinov, E. W. Collings, M. D. Sumption and H. K. Liu, *Physica C*, 2001, **361**, 79.
307 C. U. Jung, M. S. Park, W. N. Kang, M. S. Kim, S. Y. Lee and S. I. Lee, *Physica C*, 2001, **353**, 162.
308 H. D. Yang, J. Y. Lin, F. H. Hsu, C. J. Liu, S. C. Li, R. C. Yu and C. Q. Jin, *Phys. Rev. Lett.*, 2001, **8716**, 7003.
309 A. Kohen and G. Deutscher, *Phys. Rev. B*, 2001, **6406**, 506.
310 H. J. Kim, W. N. Kang, E. M. Choi, M. S. Kim, K. H. P. Kim and S. I. Lee, *Phys. Rev. Lett.*, 2001, **87**, 870021.
311 C. B. Eom, M. K. Lee, J. H. Choi, L. J. Belenky, X. Song, L. D. Cooley, M. T. Naus, S. Patnaik, J. Jiang, M. Rikel, A. Polyanskii, A. Gurevich, X. Y. Cai, S. D. Bu, S. E. Babcock, E. E. Hellstrom, D. C. Larbalestier, N. Rogado, K. A. Regan, M. A. Hayward, T. He, J. S. Slusky, K. Inamaru, M. K. Haas and R. J. Cava, *Nature*, 2001, **411**, 558.
312 D. C. Larbalestier, L. D. Cooley, M. O. Rikel, A. A. Polyanskii, J. Jiang, S. Patnaik, X. U. Cai, D. M. Feldmann, A. Gurevich, A. A. Squitieri, M. T. Naus, C. B. Eom, E. E. Hellstrom, R. J. Cava, K. A. Regan, N. Rogado, M. A. Hayward, T. He, J. S. Slusky, P. Khalifah, K. Inumaru and M. Hass, *Nature*, 2001, **410**, 186.
313 D. K. Finnemore, J. E. Ostenson, S. L. Bud'ko, G. Lapertot and P. C. Canfield, *Phys. Rev. Lett.*, 2001, **86**, 2420.
314 K. Kawano, J. S. Abell, M. Kambara and D. A. Cardwell, *Appl. Phys. Lett.*, 2001, **79**, 2216.
315 M. Dhalle, P. Toulemonde, C. Beneduce, N. Musolino, M. Decroux and R. Flukiger, *Physica C*, 2001, **363**, 155.
316 S. X. Dou, P. N. Mikheenko, X. L. Wang and H. K. Liu, *Annu. Rep. Prog. Chem, Sect. C.*, 1997, **93**, 363.
317 X. Y. Cai, A. Polyanski, Q. Li, G. N. Riley and D. C. Larbalestier, *Nature*, 1998, **392**, 906.
318 Y. C. Guo, W. M. Chen, H. K. Liu, S. X. Dou and A. V. Lukashenko, *Physica C*, 2001, **355**, 163.
319 S. X. Dou, X. L. Wang, Y. C Guo, Q. Y. Hu, P. Mikheenko, J. Horvat, M. Ionescu and H. K. Liu, *Supercond. Sci. Technol.*, 1997, **10**, A52.
320 S. X. Dou, Y. C. Guo, D. Marinaro, J. W. Boldeman, J. Horvat, P. Yao, R. Weinstein, A. Gandni, R. Sawh and Y. Ren, *Advances In Cryogenic Engineering Materials*, ed. J. Cave, Plenum Press, New York, 2000, p. 761.
321 R. Weinstein, Y. Ren, J. Liu, I. G. Chen, R. Sawh, C. Foster and V. Obot, *Proceedings of the International Workshop on Superconductivity*, Kyoto, Japan, 1994, p. 39.
322 D. Milliken and S. X. Dou, *Physica C*, 2000, **341–348**, 1411.
323 D. Milliken, J. H. Ahn and S. X. Dou, *Physica C*, 2001, **354**, 183.
324 G. W. Schulz, C. Klein, H. W. Weber, S. Moss, R. Zeng, S. X. Dou, R. Sawh, Y. Ren and R. Weinstein, *Appl. Phys. Lett.*, 1998, **73**, 3935.
325 S. X. Dou, *Physica C*, 2000, **341–348**, 2535.
326 A. V. Pan, M. H. Ionescu and S. X. Dou, *IEEE Trans. Appl. Supercond.*, 1997, **7**, 1331 and references therein.
327 M. Majoros, B. A. Glowacki and A. M. Campbell, *Supercond. Sci. Technol.*, 2001, **14**, 353.
328 G. Strano, A. S. Siri and G. Grasso, *Supercond. Sci. Technol.*, 2000, **13**, 1470.
329 A. V. Bobyl, D. V. Shantsev, T. H. Johansen, M. Baziljevich, Y. M. Galperin and M. E. Gaevski, *Supercond. Sci. Technol.*, 2000, **13**, 183.
330 M. Polak, M. Majoros, A. Kasztler and H. Kirchmayr, *IEEE Trans. Appl. Supercond.*, 1999, **9**, 2151.
331 A. V. Volkozub, J. Everett, G. Perkins, P. Buscemi, A. D. Caplin, M. Dhallé, F. Marti, G. Grasso, Y. B. Huang and R. Flükiger, *IEEE Trans. Appl. Supercond.*, 1999, **9**, 2147.
332 B. A. Glowacki, M. Majoros, M. Vickers, J. E. Evetts, Y. Shi and I. McDougall, *Supercond. Sci. Technol.*, 2001, **14**, 193.
333 G. Grasso, A. Malagoli, C. Ferdeghini, S. Roncallo, V. Braccini, A. S. Siri and M. R. Cimberle, *Appl. Phys. Lett.*, 2001, **79**, 230.
334 S. Jin, H. Mavoori and R. B. van Dover, *Nature*, 2001, **411**, 563.

335 S. Zhou, A. V. Pan, M. Ionescu, H. Liu and S. Dou, *Supercond. Sci. Technol.*, 2002, **15**, 236.
336 S. Soltanian, X. L. Wang, I. Kusevic, E. Babic, A. H. Li, M. J. Qin, J. Horvat, H. K. Liu, E. W. Collings, E. Lee, M. D. Sumption and S. X. Dou, *Physica C*, 2001, **361**, 84.
337 X. L. Wang, S. Soltanian, J. Horvat, A. H. Liu, M. J. Qin, H. K. Liu and S. X. Dou, *Physica C*, 2001, **361**, 149.
338 S. X. Dou, X. L. Wang, J. Horvat, D. Milliken, A. H. Li, K. Konstantinov, E. W. Collings, M. D. Sumption and H. K. Liu, *Physica C*, 2001, **361**, 79.
339 W. N. Kang, H. J. Kim, E. M. Choi, C. U. Jung and S. I. Lee, *Science*, 2001, **292**, 1521.
340 J. Horvat, X. L. Wang, S. Soltanian and S. X. Dou, *Appl. Phys. Lett.*, 2002, **80**, 829.
341 A. Goyal, *J. Met., Miner. Mater.*, 1995, **47**, 55.
342 R. Hawsey and J. Daley, *J. Met. Miner. Mater.*, 1995, **47**, 56.
343 W. E. Brockenborough and A. P. Malozemoff, *J. Met. Miner. Mater.*, 1995, **47**, 59.
344 K. I. Sata, *J. Met. Miner. Mater.*, 1995, **47**, 65.
345 A. Goyal, D. P. Norton, J. D. Budai, M. Paranthaman, E. D. Specht, D. M. Kroeger, D. K. Christen, Q. He, B. Saffian, F. A. List, D. F. Lee, P. M. Martin, C. E. Klabunde, E. Hartfield and V. K. Sikka, *Appl. Phys. Lett.*, 1996, **69**, 1795.
346 K. Wasa and S. Hayakawa, *Handbook of Sputter Deposition Technology*, Noyes Publications, New Jersey, 1992.
347 *Concise Encyclopedia of Magnetic and Superconducting Materials*, ed. J. E. Evetts, Permagon Press, New York, 1992.
348 H. Kung, S. R. Foltyn, P. N. Arendt and M. P. Maley, *IEEE Trans. Appl. Supercond.*, 1999, **9**, 2034.
349 C. Park, D. P. Norton, D. K. Christen, D. T. Verebelyi, R. Feenstra, J. D. Budai, A. Goyal, D. F. Lee, E. D. Specht, D. M. Kroeger and M. Paranthaman, *IEEE Trans. Appl. Supercond.*, 1999, **9**, 2276.
350 C. Varanasi, R. Biggers, I. Maartense, T. L. Peterson, J. Solomon, E. K. Moser, D. Dempsey, J. Busbee, D. Liptak, G. Kozlowski, R. Nekkanti and C. E. Oberly, *Physica C*, 1998, **297**, 262.
351 X. D. Wu, S. R. Foltyn, P. Arendt, J. Townsend, I. H. Campbell, P. Tiwari, Q. X. Jia, J. O. Willis, M. P. Maley, J. Y. Coulter and D. E. Peterson, *IEEE Trans. Appl. Supercond.*, 1995, **5**, 2001.
352 I. Yasuhiro and K. Matsumoto, *Supercond. Sci. Technol.*, 2000, **13**, 68.
353 I. Hirabayashi, Y. Yoshida, Y. Yamada, Y. Koike and K. Matsumoto, *IEEE Trans. Appl. Supercond.*, 1999, **9**, 1979.
354 A. Ichinose, A. Kikuchi, K. Tachikawa and S. Akita, *Physica C*, 1998, **302**, 51.
355 T. A. Gladstone, J. C. Moore, B. M. Henry, S. Speller, C. J. Salter, A. J. Wilkinson and C. R. M. Grovenor, *Supercond. Sci. Technol.*, 2000, **13**, 1399.
356 C. F. Liu, X. Wu, F. Y. Wang, Z. J. Yang, Y. Feng, P. X. Zhang, X. Z. Wu and L. Zhou, *IEEE Trans. Appl. Supercond.*, 1999, **9**, 1471.
357 J. O. Willis, P. N. Arendt, S. R. Foltyn, Q. X. Jia, J. R. Groves, R. F. DePaula, P. C. Dowden, E. J. Peterson, T. G. Holesinger, J. Y. Coulter, M. Ma, M. P. Maley and D. E. Peterson, *Physica C*, 2000, **335**, 73.
358 M. Ionescu, M. Lackenby, D. Dunne and S. X. Dou, *Physica C, submitted.*
359 S. Oh, J. Yoo, K. Lee, J. Kim and D. Youm, *Physica C*, 1998, **308**, 91.
360 C. Y. Yang, S. E. Babcock, A. Goyal, M. Paranthaman, F. A. List, D. P. Norton, D. M. Kroeger and A. Ichinose, *Physica C*, 1998, **307**, 87.
361 D. Q. Shi, M. Ionescu, J. McKinnon and S. X. Dou, *Physica C*, 2001, **356**, 304.
362 K. Matsumoto, S. B. Kim, J. G. Wen, I. Hirabayashi, T. Watanabe, N. Uno and M. Ikeda, *IEEE Trans. Appl. Supercond.*, 1999, **9**, 1539.
363 D. Q. Shi M. Ionescu and S. X. Dou, in *Proceedings of the International Cryogenic Materials Conference, Madison, WI, USA, July 2001*, to be published in *Adv. Cryog. Eng.*, vol. 48.
364 D. Dimos, P. Chaudhari, J. Mannhart and F. K. LeGoues, *Phys. Rev. Lett.*, 1998, **61**, 219.
365 R. W. K. Honeycombe, *The Plastic Deformation of Metals*, Edward Arnold, London, 1984.
366 F. J. Humphreys and M. Hatherly, *Recrystallisation and Related Annealing Phenomena*, Elsevier, New York, 1996.
367 R. D. Doherty, I. Samajdar, C. T. Necker, H. E. Vatne and E. Nes, *Proceedings of the 16th Risø International Symposium on Materials Science: Microstructural and Crystallographic Aspects of Recrystallisation*, Riso National Laboratory, Roskilde, Denmark, 1995, p. 1.
368 T. A. Gladstone, J. C. Moore, A. J. Wilkinson and C. R. M. Grovenor, *IEEE Trans. Appl. Supercond.*, 1999, **9**, 2252.
369 L. E. Samuels, *Metallographic Polishing by Mechanical Methods*, Sir Isaac Pitman and Sons, Melbourne, 1971.
370 V. D. Scott and H. Wilman, *Proc. R. Soc. London, Ser. A*, 1958, **247**, 353.
371 C. L. H. Thieme, S. Flesher, D. M. Buczek, M. Jowett, L. G. Fritzemeier, P. N. Arendt, S. R. Foltyn, J. Y. Coulter and J. O. Willis, *IEEE Trans. Appl. Supercond.*, 1999, **9**, 1494.
372 J. D. Budai, R. T. Young and B. S. Chao, *Appl. Phys. Lett.*, 1993, **62**, 1836.
373 J. J. Wells, J. L. MacManus-Driscoll, J.-Y. Genoud, H. L. Suo, E. Walker and R. Flükiger, *Supercond. Sci. Technol.*, 2000, **13**, 1390.
374 T. Doi, N. Sugiyama, T. Yuasa, T. Ozawa, K. Higashiyama, S. Kikuchi and K. Osamura, in *Advances in Superconductivity*, ed. H. Hayakawa and Y. Enomoto, Springer, Tokyo, 1996, vol. 8.

375 W. Mao, *J. Mater. Eng. Perform.*, 1999, **8**, 556.
376 T. Petrisor, V. Boffa, G. Celentano, L. Ciontea, F. Fabbri, U. Gambardella, S. Ceresara and P. Scardi, *IEEE Trans. Appl. Supercond.*, 1999, **9**, 2256.
377 T. G. Truchan, F. H. Rountree, M. T. Lanagan, S. M. McClellan, D. J. Miller, K. C. Goretta, M. Tomsic and R. Foley, *IEEE Trans. Appl. Supercond.*, 2000, **10**, 1130.
378 H. Makita, S. Hanada and O. Izumi, *Acta Metall.*, 1998, **36**, 403.
379 D. P. Norton, A. Goyal, J. D. Budai, D. K. Christen, D. M. Kroeger, E. D. Specht, Q. He, B. Saffian, M. Paranthaman, C. E. Klaubunde, D. F. Lee, B. C. Sales and F. A. List, *Science*, 1996, **274**, 755.
380 A. Goyal, D. P. Norton, D. M. Kroeger, D. K. Christen, M. Paranthaman, E. D. Specht, J. D. Budai, Q. He, B. Saffian, F. A. List, D. F. Lee, E. Hatfield, P. M. Martin, C. E. Klabunde and J. Mathis, *J. Mater. Res.*, 1997, **12**, 2924.
381 C. Park, D. P. Norton, D. F. Lee, D. T. Verebelyi, A. Goyal, D. K. Christen and J. D. Budai, *Physica C*, 2000, **341**, 2481.
382 S. Sathyamurthy and K. Salama, *Physica C*, 2000, **341**, 2479.
383 F. Fabbri, C. Annino, V. Boffa, G. Celentano, L. Ciontea, U. Gambardella, G. Grimaldi, A. Mancini and T. Petrisor, *Physica C*, 2000, **341**, 2503.
384 S. R. Foltyn, Q. X. Jia, P. N. Arendt, L. Kinder, Y. Fan and J. F. Smith, *Appl. Phys. Lett.*, 1999, **75**, 3691.
385 T. Aytug, M. Paranthaman, B. W. Kang, S. Sathyamurthy, A. Goyal and D. K. Christen, *Appl. Phys. Lett.*, 2001, **79**, 2205.
386 Q. Li, W. Zang, U. Schoop, M. W. Rupich, S. Annavarapu, D. T. Verebelyi, C. L. H. Thieme, V. Prunier, X. Cui, M. D. Teplitsky, L. G. Fritzemeier, G. N. Riley, M. Paranthaman, A. Goyal, D. F. Lee and T. G. Holesinger, *Physica C*, 2001, **357**, 987.
387 Y. Iijima, N. Tanabe, O. Kohno and Y. Ikeno, *Appl. Phys. Lett.*, 1992, **60**, 769.
388 Y. Iijima, K. Onable, N. Futaki, N. Sadakata and O. Kohno, *J. Appl. Phys.*, 1993, **74**, 1905.
389 R. P. Reade, P. Berdahl, R. E. Rosso and S. M. Garrison, *Appl. Phys. Lett.*, 1992, **61**, 2231.
390 X. D. Wu, S. R. Foltyn, P. N. Arendt, W. R. Blumenthal, I. H. Campbell, J. D. Cotton, J. Y. Coulter, W. L. Hults, M. P. Maley, H. F. Safar and J. L. Smith, *Appl. Phys. Lett.*, 1995, **67**, 2397.
391 Y. Nakamura, N. Hobara, K. Kakimoto, T. Izumi and Y. Shiohara, *Physica C*, 2000, **341**, 2323.
392 Y. Iijima, M. Kimura, T. Saitoh and K. Takeda, *Physica C*, 2000, **335**, 15.
393 C. P. Wang, K. B. Do, R. M. Beasley, T. H. Geballe and R. H. Hammond, *Appl. Phys. Lett*, 1997, **71**, 2955.
394 M. P. Chudzik, R. A. Erck, Z. P. Luo, D. J. Miller, U. Balachandran and C. R. Kannewurf, *Physica C*, 2000, **341**, 2483.
395 Y. Shiohara and N. Hobara, *Physica C*, 2000, **341**, 2521.
396 U. Balachandran, personal communication, 2001.
397 S. R. Foltyn, P. N. Arendt, R. F. DePaula, P. C. Dowden, J. Y. Coulter, J. R. Groves, L. N. Haussamen, L. P. Winston, Q. X. Jia and M. P. Maley, *Physica C*, 2000, **341**, 2305.
398 A. Ignatiev, P. C. Chou, Y. Chen, X. Zhang and Z. Tang, *Physica C*, 2000, **341**, 2309.
399 A. Usoskin, K. Sturn, J. Knoke, A. Issaev, F. Garcia-Moreno, J. Dzick and H. C. Freyhardt, *IEEE Trans. Appl. Supercond.*, 2001, **11**, 3385.
400 Y. Yamada, S. Kim, T. Araki, Y. Takahashi, T. Yuasa, H. Kurosaki, I. Hihabayashi, Y. Iijima and K. Takeda, *Physica C*, 2001, **357**, 1007.
401 B. Ma, M. Li, Y. A. Jee, R. E. Koritala, B. L. Fisher and U. Balachandran, *Physica C*, 2002, **366**, 270.
402 A. P. Bramley, J. D. O'Connor and C. R. M. Grosvenor, *Supercond. Sci. Technol.*, 1999, **12**, 57.
403 C. J. Stevens, C. R. M. Grosvenor and D. J. Edward, *Supercond. Sci. Technol.*, 2000, **13**, 31.
404 A. I. Braginski, *IEEE Trans. Appl. Supercond.*, 1999, **9**, 2825.
405 J. C. Ginefri, L. Darasse and P. Crozat, *Magn. Reson. Med.*, 2001, **45**, 376.
406 A. J. Kreisler and A. Gaugue, *Supercond. Sci. Technol.*, 2000, **13**, 1235.
407 Y. Zhang, *IEEE Trans. Appl. Supercond.*, 2001, **11**, 1038.
408 M. Klauda, T. Kässer, B. Mayer, C. Neumann, F. Schnell, B. Aminov, A. Baumfaulk, H. Chalopuka, S. Kolesov, H. Piel, N. Klein, S. Schornstein and M. Bareiss, *IEEE Trans. Microwave Theory Tech.*, 2000, **48**, 1227.
409 T. M. Taylor, *IEEE Trans. Appl. Supercond.*, 1999, **9**, 412.
410 P. Vase, R. Flukiger, M. Leghissa and B. Glowacki, *Supercond. Sci. Technol.*, 2000, **13**, 71.
411 D. Larbalestier, A. Gurevich, D. M. Feldmann and A. Polyanskii, *Nature*, 2001, **414**, 368.
412 W. V. Hassenzahl, *IEEE Trans. Appl. Supercond.*, 2001, **11**, 1447.
413 V. Jung, *Adv. Eng. Mater.*, 2001, **3**, 319.
414 H. Fujimoto and H. Kamijo, *Physica C*, 2001, **357**, 852.
415 I. G. Chen and J. M. Lin, *IEEE Trans. Appl. Supercond.*, 2001, **11**, 2038.
416 E. M. Leung and B. Burley, *IEEE Power Eng. Rev.*, 2000, **20**, 15.
417 H. Kumakura, *Supercond. Sci. Technol.*, 2000, **13**, 34.
418 J. Boehm, *IEEE Trans. Appl. Supercond.*, 2000, **10**, 710.
419 G. Morrow, *IEEE Trans. Appl. Supercond.*, 2000, **10**, 744.
420 W. V. Hassenzahl, *IEEE Power Eng. Rev.*, 2000, **20**(5), 4.
421 J. X. Jin, S. X. Dou, H. K. Liu, R. Neale, N. Attwood, G. Grigg, T. Reading and T. Beales, *IEEE Trans. Appl. Supercond.*, 1999, **9**, 394.

422 J. X. Jin, H. K. Liu, R. Zeng and S. X. Dou, *Physica C*, 2000, **341–348**, 2611.
423 W. V. Hassenzahl, *IEEE Power Eng. Rev.*, 2000, **20**(6), 4.
424 S. H. Kim, W. S. Kim, S. Y. Hahn and G. Cha, *IEEE Trans. Appl. Supercond*, 2001, **11**, 1968.
425 J. X. Jin, S. X. Dou, F. Darmann, M. Apperley and T. Beales, *Physica C*, 2000, **341–348**, 1601.
426 S. P. Hornfeldt, *Physica C*, 2000, **341**, 2531.
427 C. T. Reis, S. P. Mehta, B. W. McConnell and R. H. Jones, *Proceedings of the 2001 Winter Meeting of the IEEE Power Engineering Society*, Columbus, OH, 200, IEEEPiscatawny, NJ, 2001, p. 432.
428 L. K. Kovalev, K. V. Iliushin, V. T. Penkin, K. L. Kovalev, S. M. A. Koneev, K. A. Modestov, S. A. Larionoff, W. Gawalek and B. Oswald, *Physica C*, 2001, **357–360**, 860.
429 D. Driscoll, V. Dombrovski and B. Zhang, *IEEE Power Eng. Rev.*, 2000, **20**, 12.
430 J. O. Willis, *IEEE Power Eng. Rev.*, 2000, **20**(8), 10.
431 X. Jiang, X. Chu, X. Wu, W. Liu, Y. Lai, Z. Wang, Y. Dai and H. Lan, *IEEE Trans. Appl. Supercond.*, 2001, **11**, 1765.
432 J. X. Jin, X. K. Fu, H. K. Liu and S. X. Dou, *Physica C*, 2000, **341–348**, 2621.